Geophysical Journal International

Geophys. J. Int. (2012) **189,** 1237–1252 doi: 10.1111/j.1365-246X.2012.05392.x

Crustal structure and seismotectonics of central Sicily (southern Italy): new constraints from instrumental seismicity

Tiziana Sgroi,[1] Rita de Nardis[2,3] and Giusy Lavecchia[3]

[1] *Istituto Nazionale di Geofisica e Vulcanologia, Rome, Italy. E-mail: tiziana.sgroi@ingv.it*
[2] *Dipartimento della Protezione Civile, Via Vitorchiano, Rome, Italy*
[3] *Dipartimento di Scienze Umanistiche e della Terra, Università 'G. D'Annunzio', Campus Universitario,* 66013 *Chieti Scalo, Italy*

Accepted 2012 January 23. Received 2012 January 20; in original form 2011 May 26

SUMMARY

In this paper, we propose a new model of the crustal structure and seismotectonics for central Sicily (southern Italy) through the analysis of the depth distribution and kinematics of the instrumental seismicity, occurring during the period from 1983 to 2010, and its comparison with individual geological structures that may be active in the area. The analysed data set consists of 392 earthquakes with local magnitudes ranging from 1.0 to 4.7. We defined a new, detailed 1-D velocity model to relocate the earthquakes that occurred in central Sicily, and we calculated a Moho depth of 37 km and a mean V_P/V_S ratio of 1.73. The relocated seismic events are clustered mainly in the area north of Caltanissetta (e.g. Mainland Sicily) and in the northeastern sector (Madonie Mountains) of the study area; only minor and greatly dispersed seismicity is located in the western sector, near Belice, and along the southern coast, between Gela and Sciacca. The relocated hypocentral distribution depicts a bimodal pattern: 50 per cent of the events occur within the upper crust at depths less than ∼16 km, 40 per cent of the events occur within the middle and depth crust, at depths between 16 and 32 km, and the remaining 10 per cent occur at subcrustal depths. The energy release pattern shows a similar depth distribution.

On the basis of the kinematic analysis of 38 newly computed focal plane solutions, two major geographically distinct seismotectonic domains are distinguished: the Madonie Mountain domain, with prevalent extensional and extensional-oblique kinematics associated with upper crust Late Pliocene–Quaternary faulting, and the Mainland Sicily domain, with prevalent compressional and compressional-oblique kinematics associated with thrust faulting, at mid to deep crust depth, along the north-dipping Sicilian Basal Thrust (SBT). The stress inversion of the Mainland Sicily focal solutions integrated with neighbouring mechanisms available in the literature highlights a regional homogeneous compressional tensor, with a subhorizontal NNW–SSE-striking σ_1 axis. In addition, on the basis of geodetic data, the Mainland Sicily domain may be attributed to the SSE-ward thrusting of the Mainland Sicily block along the SBT plane. Seismogenic shearing along the SBT at mid-crustal depths was responsible for the unexpected Belice 1968 earthquake (M_w 6.1), with evident implications in terms of hazard assessment.

Key words: Seismicity and tectonics; Continental tectonics: compressional; Dynamics: seismotectonics; Crustal structure; Europe.

1 INTRODUCTION

The Sicilian region represents a portion of the Apennine–Maghrebide fold-and-thrust belt (Fig. 1a) developed in an area dominated by both the convergence between the European and Nubia (northern Africa) plates and the extensional-compressional processes linked to the opening of the Tyrrhenian basin. The compressional belt comprises southward-verging crustal-scale tectonic units and related back-thrusts that have been progressively overthrust since Oligocene times (Ghisetti & Vezzani 1984; Butler *et al.* 1992; Lentini *et al.* 1994; Catalano *et al.* 1996; Guarnieri *et al.* 2002; Tavarnelli *et al.* 2003). The outermost and youngest group of tectonic units consists of late Pliocene–Quaternary south-verging fold-and-thrust structures developed at the hanging wall of a major north-dipping thrust discontinuity (Sicilian Basal Thrust, SBT; in Lavecchia *et al.* 2007a), whose surface tip line extends with a southward arcuate shape from Sciacca to Gela and Catania (Fig. 1a). Active and

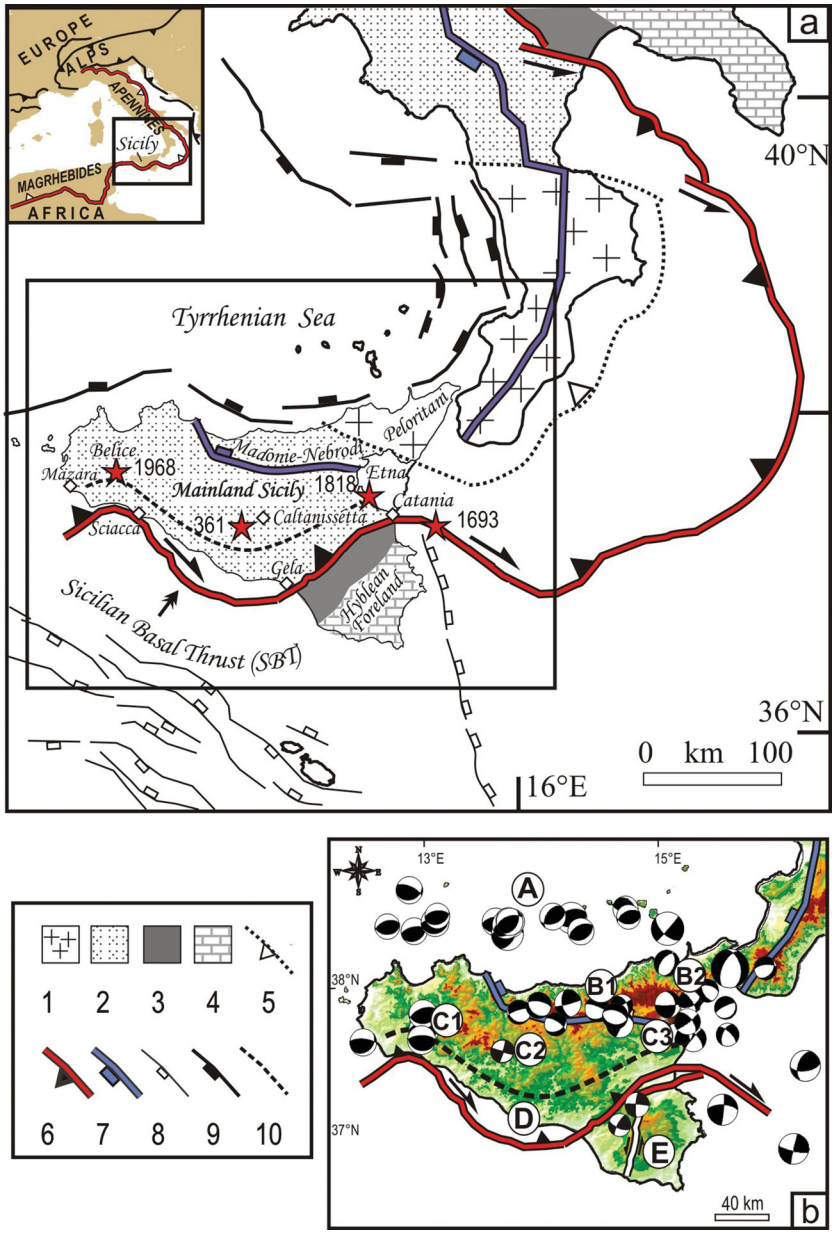

Figure 1. (a) Tectonic framework of the study area with the major structural domains of southern Italy (from Lavecchia *et al.* 2007a). Key: (1) Calabria–Peloritani metamorphic thrust units; (2) Apennine–Maghrebide early Miocene to Quaternary fold-and-thrust system; (3) Plio-Quaternary deformed foredeep deposits; (4) Hyblean and Apulian foreland; (5) thrust front of the Alpine-derived Calabria–Peloritani units; (6) Outer thrust front of the Apennine–Maghrebide chain; (7) Outer extensional front of the intra-Apennine and Sicilian, Plio-Quaternary normal and normal-oblique faults; (8) Sicily Channel normal fault system and Malta Escarpment fault trace; (9) Tyrrhenian Sea normal faults; (10) southern boundary of the Mainland Sicily active compressional domain. The red stars refer to major Sicilian historical earthquakes ($M_w \geq 6$; Working Group CPTI 2004). (b) Fault plane solutions mechanisms for events with $M_w \geq 4$ in the period 1978–2010 at depths ≤40 km (Pondrelli *et al.* 2006 and references therein; RCMT database available online at http://www.bo.ingv.it/RCMT/Italydataset.html) integrated with the Belice 1968 and Reggio Calabria 1908 focal mechanisms as reported by Anderson & Jackson (1987). Five seismotectonic domains are labelled, from north to south: (A) southern Tyrrhenian compressive domain; (B) northern Sicily extensional domain including the Madonie-Nebrodi (B1) and the Peloritani (B2) areas; (C) mainland Sicily compressive domain, including the Mazara-Belice (C1), Caltanissetta (C2) and Etna (C3) areas; (D) Southern Sicily compressive domain from Sciacca to Gela and Catania and (E) Hyblean Foreland strike slip domain.

possibly seismogenic compression of the SBT and its hanging wall splays in Quaternary times is debated. Some investigators assume cessation of active convergence since early middle Pleistocene times (Butler *et al.* 1992; Torelli *et al.* 1998; D'Agostino & Selvaggi 2004; Ghisetti *et al.* 2009); others consider the SBT still active (Catalano *et al.* 2004; Jenny *et al.* 2006; Lavecchia *et al.* 2007a).

Historical and instrumental seismic data support the seismogenic compression hypothesis as it relates to the western (Monaco *et al.* 1996; Anderson & Jackson 1987; Pondrelli *et al.* 2006) and eastern regions of Sicily (Cocina *et al.* 1997; Neri *et al.* 2005; Lavecchia *et al.* 2007a and references therein), whereas no seismotectonic information is available on the active state of strain in central Sicily, specifically in the area of Caltanissetta (Fig. 1a). Such portion of

Sicily, hereinafter named Mainland Sicily (Fig. 1a), appears as an aseismic domain in the most recent official seismic zoning of the Italian territory (model ZS9 in Meletti *et al.* 2008) and in the corresponding individual seismic source model (Basili *et al.* 2008). This appearance as an aseismic domain is due mainly to three different observations: (i) since early instrumental times, Mainland Sicily has not been struck by a significant earthquake; (ii) the background seismicity recorded over the past 20 yr was low and infrequent, and (iii) the seismic station coverage was less favourable with respect to other Italian areas.

The aim of this work is to clarify the active state of strain and evaluate the seismogenic sources in central Sicily through the investigation of the geometry and kinematics of the potentially active sources. The first part of the paper aims to improve and extend the knowledge on hypocentre locations occurring in the study area. The collection of seismic recordings related to 392 local earthquakes ($1.0 \leq M_L \leq 4.7$) occurred in the period from 1983 to 2010, and the creation of a joint data set composed of both arrival times from national bulletins (time interval 1983–2005) and repicked seismic data (time interval 2005–2010) was performed. To create a uniform starting seismic catalogue, the joint data set was preliminarily relocated using an 1-D velocity model optimized for the Italian territory (Chiarabba *et al.* 2005). Subsequently, a new 1-D velocity model was computed for central Sicily and was used to perform the final relocation of the whole data set. The second part of the study is dedicated to the calculation of first motion polarity focal mechanisms and to the tectonic interpretation. The new focal mechanisms are integrated with fault solutions from the literature to better constrain the seismotectonic regime of the region. The obtained results provide further insight into the regional state of stress of the SBT and surrounding regions.

2 SEISMOTECTONIC FRAMEWORK

On the basis of evidence from fault plane solution mechanisms of moderate-to-large crustal earthquakes ($M_w \geq 4.0$, depth ≤ 40 km; Neri *et al.* 2005; Lavecchia *et al.* 2007a; Billi *et al.* 2010; Visini *et al.* 2010), five major geographically and kinematically seismogenic domains may be distinguished in Sicily. They are shown schematically in Fig. 1(b). From north to south, they are: (A) the Southern Tyrrhenian E–W striking domain, located off-shore of northern Sicily, undergoing N–S compression; (B) the northern Sicily domain including the Madonie-Nebrodi (B1) and the Peloritani (B2) areas, undergoing N–S and WNW–ESE tension, respectively; (C) the Mainland Sicily domain undergoing primarily nearly N–S compression in the Mazara-Belice (C1) and Etna areas (C3) and strike-slip deformation in the Caltanissetta area (C2); (D) the southern Sicily domain, extending from Sciacca to Gela and Catania, not associated with any significant instrumental earthquake and (E) the Hyblean Foreland domain in southeastern Sicily with primarily strike-slip deformation.

Although some seismological studies have been performed in the Madonie–Nebrodi–Peloritani and Hybleans domains (e.g. Musumeci *et al.* 2003; Langer *et al.* 2007), no direct information concerning the velocity structures and kinematics in the Mainland Sicily domain is available. Neri *et al.* (2005) and Jenny *et al.* (2006) identify a unique large province, inclusive of the Mainland Sicily and Southern Tyrrhenian domains, undergoing NNW–SSE compression. Lavecchia *et al.* (2007a) interpreted Mainland Sicily as an independent seismogenic province undergoing N–S compression at mid-crustal depths, at the hangingwall of the N-dipping SBT. The shallower upper crustal portion of the SBT province has an arcuate shape at surface and coincides with the Sciacca–Gela–Catania thrust front (Fig. 1a). Wells and seismic reflection profiles reveal the uppermost few kilometres of the SBT downdip geometry (Lickorish *et al.* 1999), while at depth, the geometry may be only inferred. A thick-skinned style is proposed by some authors (Guarnieri *et al.* 2002; Lavecchia *et al.* 2007a), and they assume a northward deepening of the SBT to depths of nearly 35–40 km beneath central and northern Sicily.

Although Mainland Sicily is not considered an active seismogenic zone, three large historical earthquakes ($M_w \geq 6.0$) may be associated with thrust activity. From west to east, they are Belice 1968 (M_w 6.1), central Sicily 361 (M_w 6.6) and Catania 1818 (M_w 6.0; Fig. 1a). The 1968 earthquake occurred in the Belice area (west of Mainland Sicily), where no other significant earthquake is reported in the historical catalogue and where very scarce background seismicity is recorded, apart from the 1981 Mazara del Vallo earthquake (M_w 4.9). This event, nucleated nearly 40 km west from the Belice earthquake, was associated with N–S compression along a north-dipping thrust plane at depths of 15–20 km. On the other hand, the Belice sequence was elongated in a roughly E–W direction (Gasperini *et al.* 1999; Valensise & Pantosti 2001), and the hypocentres were distributed along a N-dipping thrust plane from near the surface to a depth of ∼30 km (Monaco *et al.* 1996). The focal solution of the main event and of two major aftershocks were evaluated as both thrusting on a north-dipping plane (Anderson & Jackson 1987) and right lateral oblique compression on a NNE-striking plane (McKenzie 1972; Gasparini *et al.* 1985). In both cases, the average *P*-axis was evaluated being nearly N–S and subhorizontal. The central area of the Mainland Sicily domain was highly damaged by the 361 earthquake (M_w 6.6), whose macroseismic epicentre was located at Caltanissetta, according to archaeological evidence of damages reported at the great historic Roman Villa of Casale in the town of Piazza Armerina (III–IV A.D.; Working Group CPTI 2004). Although some investigators attributed the event to N–S compression (Jenny *et al.* 2006; Visini *et al.* 2010), others proposed a northward relocation in the Madonie Mountains extensional area (Barreca *et al.* 2010). The eastern area of the Mainland Sicily domain was struck by the Catania 1818 (M_w 6.0) earthquake. Although located at the southern flank of Mt Etna, such events are commonly interpreted as tectonic and independent from the volcanic activity (Azzaro *et al.* 2000) and possibly associated with N–S/NNW–SSE compression (Lavecchia *et al.* 2007a).

The area located at the hangingwall of the shallowest portion of the SBT, close to the surface trace of the Sciacca–Gela–Catania thrust front, is characterized by a moderate level of seismic activity with a few events with $M_w < 5.0$ on the western side of the arc (1578, 1652, 1727, 1740, 1817, 1933) and by several events with $M_w \sim 5.5$ in the eastern side, from Gela (Fig. 2) to Mineo (1624, 1878, 1896, 1903, 1909) and Catania (1959; Working Group CPTI 2004). Not far from Sciacca, two destructive events may have occurred between the 4th and 3rd century B.C. and between the 6th and 13th century A.D. These events are indicated by archeoseismological evidence at the Selinunte temples (Guidoboni *et al.* 2002).

The historical seismic record in Sicily may be considered complete only from the 17th century (1680 ± 100) for events with $M \geq 5.5$ (Lavecchia *et al.* 2007b and references therein) and the 19th century (1825 ± 25) for events with $M \geq 4.5$. Therefore, earthquakes with longer recurrence times cannot be excluded in Mainland Sicily, and the identification of their potential seismogenic sources is important to seismic hazard assessment.

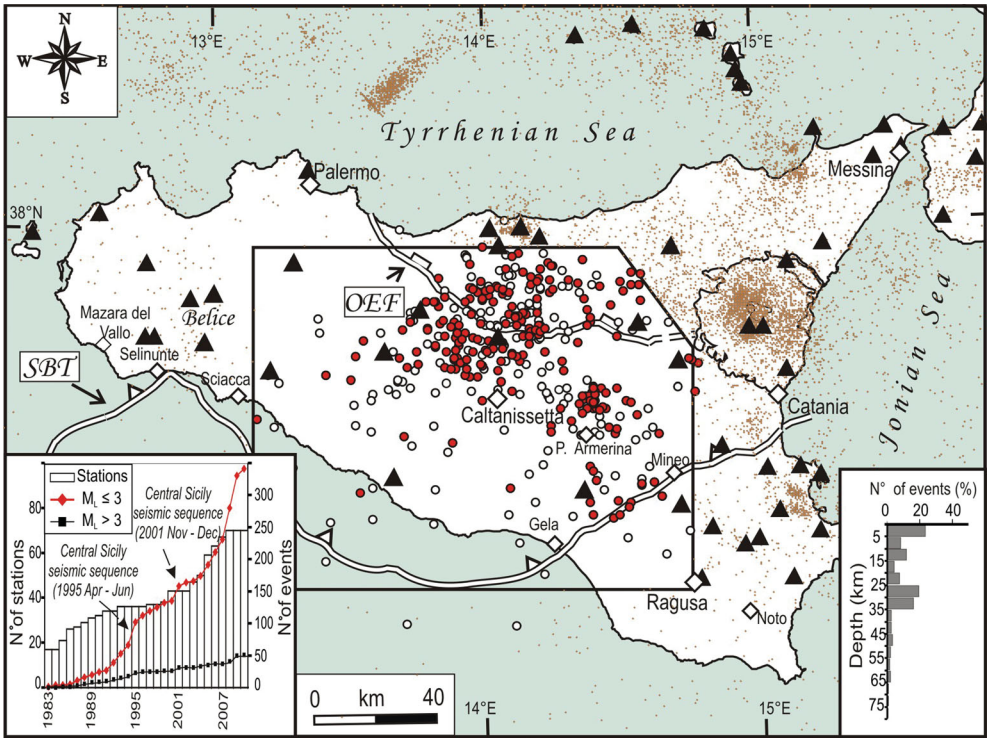

Figure 2. Preliminary relocations of 392 earthquakes (white and red circles) occurring within the central Sicily study area from 1983 to 2010 ($1.0 \leq M_L \leq 4.7$); the red circles are the epicentres of the 215 best-quality events. The brown dots represent the earthquakes that occurred in Sicily from 1983 to 2010 (Castello *et al.* 2005; ISB 2003–2010) and which were not analysed in this paper. The permanent seismic stations are reported with black triangles. The histogram within the bottom right inset shows the depth distribution of the preliminary relocated events. The diagram within the bottom left inset shows the number of seismic stations and cumulative number of earthquakes per year and per two ranges of magnitude. OEF and SBT stand for Outer Extensional Front and Sicilian Basal Thrust, respectively.

3 SEISMOLOGICAL DATA AND PROCESSING

We analyse the crustal instrumental seismicity that occurred in central Sicily between 1983 and 2010, recorded by the National Seismic Network (RSN) and managed by the Istituto Nazionale di Geofisica e Vulcanologia (INGV). The boundary of the study area is enclosed in the rectangular area outlined in Fig. 2. The RSN improved significantly over the last 5 yr throughout Italian territory and, in particular, in Sicily. An increasing number of three-component extended band (Lennartz 5 s) and/or broad-band (Trillium 40 s) sensors, replacing the Kinemetrics S-13 short period sensors, were deployed resulting in better station coverage. In 1983, the RSN had 17 stations deployed in Sicily, in the Aeolian Islands and southern Calabria; however, today, the RSN has approximately 70 stations (triangles in Fig. 2).

Following previous investigators (Amato & Mele 2008; Schorlemmer *et al.* 2010) that noted the improved earthquake detection capabilities of the national network and the lowering of the earthquake catalogue completeness threshold, we observe that the denser coverage of broad-band seismic stations in Sicily since 2005 has significantly lowered the magnitude of detectable earthquakes. This observation is well evident in the diagram within the bottom-left inset of Fig. 2, which shows the cumulative number of earthquakes recorded within the study area per year and per two ranges of magnitude ($M_L \leq 3.0$ and $M_L > 3.0$, respectively). In this figure, the two small steps indicate the occurrence of two seismic sequences in central Sicily (between 1995 April and June and between 2001 November and December), and the third one indicates the improvement of earthquake detection capabilities due to the development of seismic network and which can be seen from 2005 onward.

We collected the available arrival times of earthquakes during the period from 1983 December to 2005 April, as reported by the CSI catalogue (Castello *et al.* 2005) and by the Italian Seismic Bulletin (ISB 2003–2010; http://bollettinosismico.rm.ingv.it). However, we analysed the waveforms and repicked the arrival times of events recorded by the RSN from 2005 April to 2010 April. Similarly to the weighting procedure used for bulletin's traveltimes and on the basis of the picking accuracy, we assigned to each *P* or *S* arrival a weight, varying from 0 (accuracy of 0.05 s) to 4 (accuracy of 2.0 s or more). All *P*- and *S*-readings in single earthquakes having weights of four were excluded from the relocation procedure and from further analysis. We collected a total data set comprising 3566 *P*- and 2159 *S*-phases, associated with 392 earthquakes, with local magnitudes ranging from 1.0 to 4.7.

3.1 Preliminary relocations

To standardize the compiled data set, in terms of location procedure and quality of results, we performed a preliminary relocation using the velocity model proposed by Chiarabba *et al.* (2005) for the Italian territory and using the Hypoellipse code (Lahr 1989). The obtained epicentral distribution of events is presented in the map of Fig. 2, while their depth distribution is shown in the bottom-right side inset. In the histogram, the hypocentral depths range 0–75 km, with the majority of events located within 0–15 km and 20–35 km depth intervals.

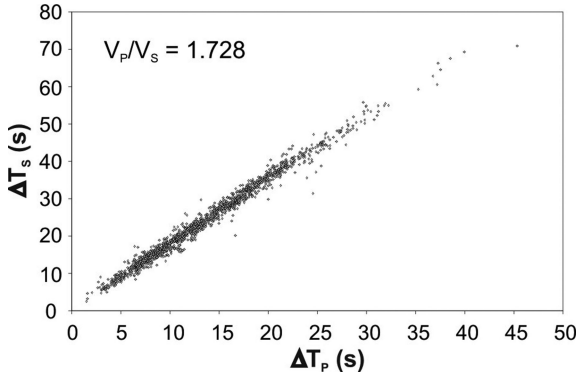

Figure 3. Cumulative Wadati diagram; the data set consists in 1565 *P*- and *S*-phase arrival times associated to 215 selected earthquakes (red circles in Fig. 2).

With the purpose of determining the V_P/V_S ratio and calculating a 1-D minimum velocity model, we selected from the total data set the events that satisfied the following requirements: (i) a minimum number of eight readings (at least five easily readable *P* and three clear *S* arrivals), (ii) maximum travel time residuals (rms) of 0.8 s and (iii) maximum GAP of 180°. In so doing, we obtained a selected data set, which consists of 215 best-constrained events (red epicentres in Fig. 2).

3.2 V_P/V_S ratio

Considering the time readings of both *P* and *S* phases from the selected database, a mean velocity ratio V_P/V_S was computed using the cumulative Wadati diagram. A V_P/V_S ratio of 1.728 with a 95 per cent confidence interval bounded by the values 1.718 and 1.739, having a squared correlation coefficient (R^2) greater than 0.98, was estimated (Fig. 3). This value of the V_P/V_S ratio is much lower than the ones found in the northern, central and southern Apennines ($V_P/V_S = 1.80$, $V_P/V_S = 1.85$, $V_P/V_S = 1.83$ and $V_P/V_S = 1.82$) from Piccinini *et al.* (2009), Monna *et al.* (2003), Bagh *et al.* (2007) and Maggi *et al.* (2010), while it is slightly lower than the values calculated by Langer *et al.* (2007) for the Calabro–Peloritan zone ($V_P/V_S = 1.75$) and the value obtained for the Hyblean Foreland by Musumeci *et al.* (2003) (average value $V_P/V_S = 1.76$).

4 MINIMUM 1-D VELOCITY MODEL

Events location in central Sicily suffers from the lack of a specific velocity model for the study area. As is well known, the use of inadequate velocity parameters during the location process can introduce systematic errors in the hypocentre location (Thurber 1992; Eberhart-Phillips & Michael 1993), which may results in incorrect seismotectonic interpretations. Therefore, the identification of a more suitable velocity model for central Sicily is necessary. As both the density of the network and the number of earthquakes do not permit 3-D tomography with an adequate resolution, we pointed to a 1-D inversion of the velocity structure.

4.1 Starting velocity models

A common problem in the inversion procedure is the dependence of the results on the initial guess. Following Kissling *et al.* (1994), we carefully chose the starting models used for the inversion of the velocity structure. Therefore, we first collected all the *a priori* available information regarding the impedance structure of Sicily (velocities and layer thickness). Seven 1-D *P*-wave velocity models were taken from the literature and sketched in Fig. 4 (from a to g). Model (a) is a regional model, computed from the analysis of seismological data recorded in central and southern Italy (Chiarabba & Frepoli 1997); it consists of four layers and assumes a Moho depth of 35 km depth for the entire Sicily region. Models (b) and (c) were computed across eastern and western Sicily by a joint interpretation of wide-angle seismic refraction profiles and Bouguer anomalies (Chironi *et al.* 2000). The eastern model (b) consists of three layers, with a Moho depth of 30 km and a sub-Moho *P*-wave velocity of 7.0 km s^{-1}; the western model (c) consists of four layers, with a Moho depth of 35 km and a sub-Moho *P*-wave velocity of 7.2 km s^{-1}. Model (d) was obtained from the integrated structural–kinematic and seismological analysis of the crustal structure in central-southern Sicily (Lavecchia *et al.* 2007a). Models (e), (f) and (g) were obtained from crustal tomography investigations in the Calabrian Arc-Sicilian region (Barberi *et al.* 2004; Billi *et al.* 2010). Among these three models, two consist of nine layers, and the third consists of eight layers, with a Moho depth at 40, 43 and 39 km and a sub-Moho *P*-wave velocity of 7.25, 7.50 and 7.25 km s^{-1}, respectively.

4.2 Minimum 1-D velocity model for central Sicily

For the identification of optimum minimum 1-D *P*-velocity model for central Sicily, we have used the widely known software VELEST (Kissling 1995). In this approach, the hypocentre locations, the velocity structure and the station corrections are derived using a simultaneous inversion of *P* and *S* waves.

The inversion was performed using the selected database of 215 events (Fig. 2) and the seven starting velocity models previously discussed (Fig. 4). *S*-wave readings were included only to better constrain the earthquake location.

We obtained the final model performing attempts by trial and error with different combinations of damping factors and by adjusting the layer thickness of the initial models (a–g in Fig. 4) to better estimate the depth of the main discontinuities. Afterwards, we further tested average models that were derived from ones we selected with different layering. In particular, we created some models with thin layers near the Moho discontinuity to constrain its depth and

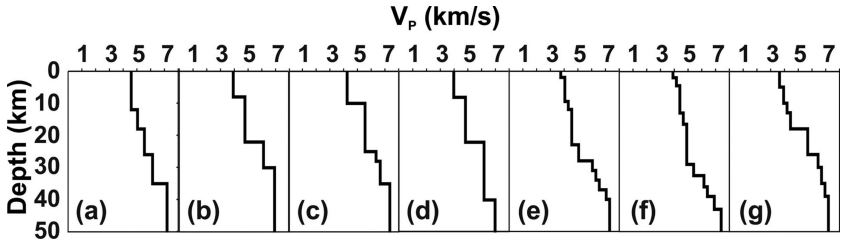

Figure 4. Compilation of *P*-wave velocity models from the literature for Sicily, computed by Chiarabba & Frepoli 1997 (model a); Chironi *et al.* 2000 (models b and c); Lavecchia *et al.* 2007a (model d), Barberi *et al.* 2004 and Billi *et al.* 2010 (models e–g).

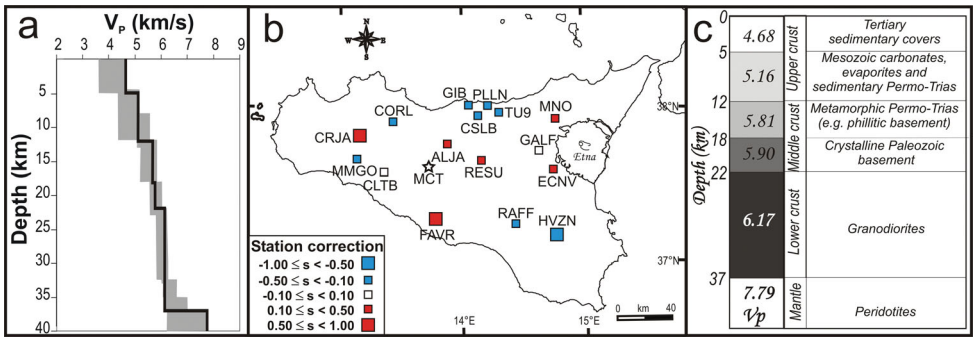

Figure 5. 1-D velocity model and crustal structure in central Sicily. (a) New 1-D velocity model (black line) calculated in this work, enclosing in the grey area representing the range of variability of the output velocity model. (b) Station corrections computed from the inversion; positive values, observed mostly in central Sicily and near the Mt Etna volcanic area indicate low velocities; negative values, observed mostly outward of the study area, indicate high velocities. (c) Lithostratigraphic interpretation of the new velocity model.

balanced opportunely the damping factors to avoid both overdamping and an unrealistic velocity model solution.

The steps that lead to the final model consisted of several inversions. For each inversion, we analysed the rms trends versus the number of iterations and chose as the best model the one corresponding to the minimum misfit of traveltime residuals. Even when we used a wide range of variability and combinations of values within each different layer (Fig. 4), the output models were quite similar, implying a stable solution. The final velocity model obtained from the inversion is sketched in Fig. 5(a) and is enclosed by the grey area, which represents the range of variability of the computed minimum 1-D velocity models with a misfit less than or equal to 0.14 s, value compatible with the noise level of traveltime data. Among these computed velocity models, the best one was chosen on the basis of goodness of the fit (0.12 s), the reduction of rms with respect to the starting and final traveltime residuals (85 per cent from 0.79 s to 0.12 s) and the *a priori* geological–geophysical information.

The new velocity model for central Sicily has five layers above the Moho, which is located at a depth of 37 km (Fig. 5a). The velocity pattern is fairly well resolved in the upper, middle and lower crust (approximately 96 per cent of the ray paths across these layers; Table 1), although the uppermost and deepest layers are also sufficiently constrained. The new 1-D velocity model shows relatively low V_P values in the upper crust (∼5.0 km s^{-1} down to 12 km) with respect to the values obtained for other parts of Italy, for example, the Apennines chain (Piccinini *et al.* 2009; Monna *et al.* 2003; Chiarabba *et al.* 2009; Bagh *et al.* 2007; Maggi *et al.* 2010), and these values are in agreement with the average velocities retrieved for the entire Sicilian region (Chiarabba & Frepoli 1997), for the Hyblean Foreland (Musumeci *et al.* 2003) and the Nebrodi–Peloritani area (Langer *et al.* 2007), where average values of 5.1, 5.2 and 4.9 were found, respectively. The Moho depth at 37 km is in agreement with the ranges of values (35–40 km) proposed by different authors (Finetti 2005; Tesauro *et al.* 2008; Grad *et al.* 2009); conversely, the velocity beneath the base of the crust (7.79 km s^{-1} at depths >37 km) is slightly greater than the average value (7.56 km s^{-1}) computed by Chiarabba & Frepoli (1997) and close to the value (8.0 km s^{-1}) derived from a DSS profile across Sicily (Cassinis *et al.* 2005).

The station corrections are positive in central Sicily, consistently associated with the thick deposits of the soft sediments of the Caltanissetta basin, while negative values are evident in northern Sicily and in the Hyblean Foreland (Fig. 5b). The positive values of the ECNV and MNO station corrections, placed near the Mt Etna volcano, correlate well with the presence of the thermal effects associated with the volcanic activity. A geological interpretation of the inferred *P*-wave velocity model of central Sicily is shown in Fig. 5(c). The low *P*-wave velocities in the upper crust might be associated with the presence of a thick Tertiary sedimentary cover in the uppermost 5 km and with Mesozoic carbonates, evaporites and sedimentary Permo-Trias terrains at depths between 5 and 12 km; a metamorphic Permo-Trias basement (from 12 to 18 km) above a crystalline Palaeozoic basement (from 18 to 22 km) might characterize the middle crust, whereas a classic granodiorite composition may be assumed for the lower crust at depths between 22 and 37 km. The *P*-wave velocities of the upper mantle (over 37 km depth) would be associated with a peridotitic composition.

Table 1. Range of velocity variation for input models, velocity values of the best model for the central Sicily computed with VELEST code and percentage of ray sampling within the layers of the best model.

Range of velocity variation for input models		Best model		
Depth range (km)	Velocity range Min – Max (km s^{-1})	Depth range (km)	Velocity (km s^{-1})	Per cent Ray sampling
0–5	3.0–5.0	0–5	4.68	22
5–10	4.0–6.0	5–12	5.16	23
10–15	4.0–6.0	12–18	5.81	18
15–20	4.0–6.0	18–22	5.90	14
20–25	4.0–7.0	22–37	6.17	19
25–30	5.0–7.0	>37	7.79	4
30–35	5.5–8.0			
35–40	5.7–8.0			
>40	7.0–8.0			

5 EARTHQUAKE FINAL RELOCATIONS

We performed the final relocations of the entire data set of 392 earthquakes that occurred in central Sicily from 1983 to 2010, using the Hypoellipse code (Lahr 1989). Considering the presence in Sicily of five well distinguished crustal and seismotectonic domains (Fig. 1b), we associated with each of them the appropriate velocity model. These models were derived from the literature (Fig. 6, and references therein), apart from the new one that is computed here for Mainland Sicily, and were applied to all the seismic stations lying within the boundary of the study area. The final epicentral relocations distribution is shown in the map of Fig. 6. We observe two

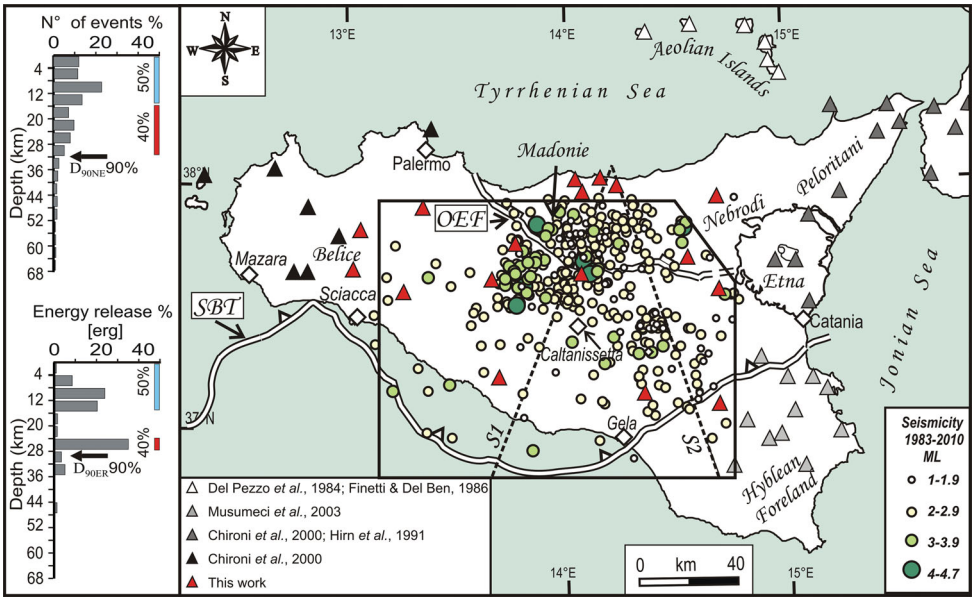

Figure 6. Final relocation of 392 earthquakes that occurred from 1983 December to 2010 April within the study area; magnitude scales are also reported. The triangles represent the seismic stations, and their colours are related to the different velocity models used for the relocation, depending on the seismotectonic domain where the stations are placed. The dotted black lines (S1 and S2) show the trace of the sections in Figs 7 and 9. The insets at the left side represent the depth distribution and the energy release versus depth of the best relocated events (quality A and B).

major concentrations of earthquakes in the northeastern sector of the study area (Madonie Mountains) and in the area north and northwest of Caltanissetta; a minor and greatly dispersed seismicity is evident in the western sector, close to the Belice valley, and along the southern coast, between Gela and Sciacca. A depth view of the seismicity is presented in Fig. 7, where the earthquakes are projected along the traces of two sections striking NNE–SSW (S1) and NNW–SSE (S2), across the study area (Fig. 6), assuming a semi-width of 20 km. The relocated hypocentres (Fig. 7C) are compared with the bulletin locations (Fig. 7A) and with the ones preliminarily relocated (Fig. 7B). An improvement of the final locations with respect to the original and preliminary ones is evident. In both sections, the original and preliminary locations show a clustering of the hypocentres at depths of approximately 13 and 34 km, respectively, probably as a result of strong discontinuities in the adopted velocity and/or fixed depths in the location procedures. Conversely, the final depth distribution does not show any systematic shift of the hypocentres, and the seismicity is distributed in a N-dipping wedge shape volume.

We estimated the quality of the final locations accounting for the azimuthal gap, the root mean square of the traveltime residuals (rms) and the horizontal (ErrH) and vertical (ErrZ) errors determination (Table 2). Hypocentral solutions with azimuthal gaps $<180^\circ$, rms < 0.5 s and ErrH and ErrZ errors lower than 1 km were considered the best location quality (A). On the other hand, hypocentral solutions with gaps $> 180^\circ$, rms > 1.0 s and ErrH and ErrZ greater than 10.0 km gave the worst locations quality (D). In total, 134 events have quality A, 221 quality B, 31 events have quality C and only 6 events are of quality D. The comparison between the quality of the preliminary relocations (Fig. 2) and the final relocations (Fig. 6) is presented in the histograms of Fig. 8. In particular, the *P*- and *S*-phase residuals (Figs 8a–a′ and b–b′), the rms residuals (Figs 8c–c′), and the horizontal and vertical errors (Figs 8d–d′ and e–e′) are compared to the number of events. Most of the final relocations have rms of less than 0.5 s and horizontal and vertical errors of less than 1 km, demonstrating the improvement in location determination. Moreover, the comparison of mean (M) and standard deviation (SD), computed on the former parameters and marked within the histograms of Fig. 8, highlights the improvement of our final location quality compared to the preliminary ones.

The hypocentral distribution of the best relocated events (quality A and B) in terms of number of events and energy release, evaluated using the magnitude–energy relationship ($\log E = 9.9 + 1.9Ml + 0.024Ml2$ valid for $M_L \leq 4.5$, Richter 1958) for classes of depths, is shown in the two histograms within the left panel of Fig. 6, which depict a bimodal pattern. The 50 per cent of events occurring at depths less than $\sim$16 km realize 50 per cent of the energy; the 40 per cent occurring at depths between 16 and 32 km realize 40 per cent of total energy at depths between 24 and 28 km.

Assuming the base of the seismogenic layer as the depth corresponding to 90 per cent of the seismicity on the cumulative curves of the total number of events (D_{90NE}) and energy release (D_{90ER}; black arrows on histograms of Fig. 6), a cut-off depth of approximately 32 km is estimated. In fact, the integration of histograms with the earthquake distribution in map and section view shows that such a value is representative only of Mainland Sicily, whereas in the northern sector of the study area (the Madonie Mountains), 90 per cent of the seismicity is shallower than 16 km (Fig. 7).

6 FOCAL MECHANISMS

The repicking process also permitted us to collect *P*-wave first motion polarities and compute focal mechanism solutions using the FPFIT standard procedure (Reasenberg & Oppenheimer 1985). We considered the polarities of all events occurring within the central Sicily study area from 1983 to 2010, and we evaluated the focal mechanisms for 60 events. From this data set, we selected 38 solutions with a minimum number of eight clear observations homogenously distributed on the focal sphere (approximately 70 per cent of events have a number of polarities ≥ 11) and with less than two discrepant polarities (approximately 60 per cent of events do not have discrepant polarities; Fig. 9). The selection was further

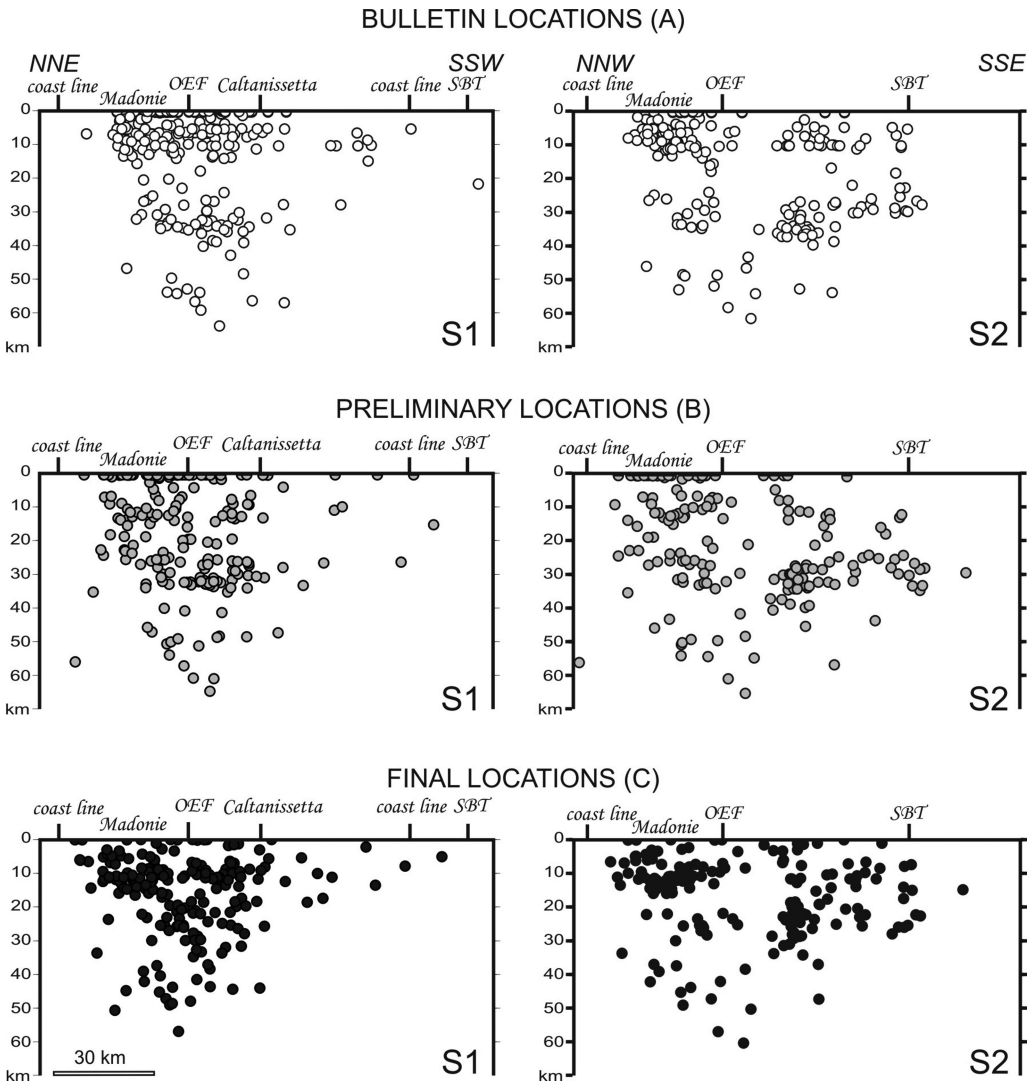

Figure 7. Section view of the 1983 December–2010 April central Sicily instrumental seismicity and projected along the traces of the S1 and S2 sections of Fig. 6, assuming a semiwidth of 20 km. Bulletin locations (A) were extracted from national seismic bulletins (Castello *et al.* 2005; ISB 2003–2010); preliminary locations (B) were obtained assuming the velocity model of Chiarabba *et al.* (2005); final locations (C) are the ones that were relocated here, using the new velocity model calculated for central Sicily and the velocity models taken from the literature for the surrounding seismotectonic domains. The positions along the profiles of the Outer Extensional Front (OEF) and of the Sicilian Basal Thrust (SBT) front are also shown.

Table 2. Location parameters: limit value for GAP, rms and horizontal and vertical errors used to determine the location quality.

Quality	GAP	rms (s)	ErrH (km)	ErrZ (km)	Number events
A	$<180°$	<0.5	<1.0	<1.0	134
B	$<180°$	0.5–1.0	1.0–5.0	1.0–5.0	221
C	180°–220°	0.5–1.0	5.0–10.0	5.0–10.0	31
D	$>220°$	>1.0	>10.0	>10.0	6

checked on the basis of the two quality factors (Q) of the FPFIT code, decreasing from A to C, which are the degree of polarity misfit (Q_p) and the range of uncertainties of strike, dip and rake (Q_f) in a solution. The focal mechanisms parameters are listed in Table 3; 13 solutions have quality A–A; 21, A–B or B–A and 4, B–B.

The relocated epicentres are projected in the map of Fig. 9(a). Eleven focal mechanisms lie within the Plio-Quaternary Madonie Mountains extensional domain (B1 in Fig. 1), northward of the Outer Extensional Front, OEF, in Fig. 9); 23 lie in the central portion of the Mainland Sicily domain (C2 in Fig. 1), which is located between the OEF and the SBT front.

Following the Frohlich (1992) classification scheme, based on the plunge of *T*-, *B*- and *P*-axes, the solutions are subdivided into five kinematic categories (thrust, thrust-strike, strike, normal, normal-strike) plus an unclassified category and are represented schematically in a ternary diagram (see the uppermost left side inset of Fig. 9a). Although the overall kinematics of the considered earthquakes are of mixed type, when considering the earthquake spatial distribution in map and in section view (Figs 9a and b), it is possible to identify three spatially distinct groups with rather homogeneous kinematics. One group is located within the Madonie Mountains domain; the other two (one prevalent, the other subordinate), in Mainland Sicily. The three groups also differ in their depth distribution, as is well highlighted by the depth histograms of Fig. 10. The Madonie Mountains group (MM in Figs 9 and 10) is characterized by seismic events ($2.0 \leq M_L \leq 4.3$) with prevalent normal and normal/oblique kinematics nucleated in the 0–15 km depth range. The Mainland Sicily prevalent group (MS1 in Figs 9 and 10) is

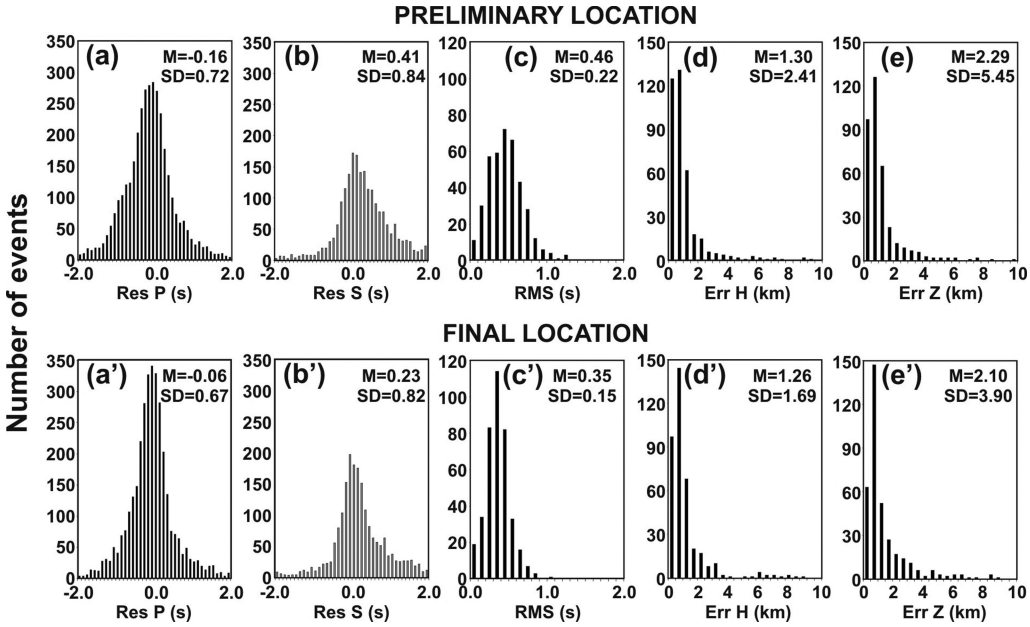

Figure 8. Comparison of quality parameters between the preliminary relocations and the final relocations; the histograms show *P*- (a and a′) and *S*-phase (b and b′) residuals, rms (seconds, c and c′), horizontal (d and d′) and vertical (e and e′) errors (kilometres) versus the number of events obtained from the preliminary and the final relocation procedure. Within each box, the values of mean (M) and standard deviation (SD) are also reported to highlight the improvement in the location procedure from the preliminary to the final locations.

characterized by seismic events ($2.1 \leq M_L \leq 4.7$) with reverse and oblique/reverse kinematics, located mainly at depths between 25 and 30 km, along the downdip projection of the N-dipping SBT plane. The Mainland Sicily minor group (MS2 in Figs 9 and 10) consists of a small cluster of low magnitude events ($2.0 \leq M_L \leq 3.1$) with a predominance of normal and oblique/normal solutions, located at depths between 15 and 25 km, within the SBT footwall.

To verify the kinematic compatibility among the population of focal mechanisms of each group, the simple right dihedral graphic construction (Angelier & Mechler 1977) was applied (Figs 10a–c). The graphic construction consists of a grid stereographic projection that indicates, at each gridpoint, the number of dihedrals delimited by the nodal planes that contain the *P*- or the *T*-axis; the necessary condition for belonging to a single stress tensor is that 100 per cent of the data fall within the area defined by the dihedral superposition. Such condition is fully satisfied for the P-dihedra grid of the MS1 group (100 per cent at one grid node) and for the T-dihedra grid of the MS2 and MM groups.

To highlight the prevailing kinematics of each group, an average focal solution was also computed by using the FaultKinWin 1.1. software (Allmendinger 2001) and by applying both the Bingham statistical procedure that does not weight the data for the seismic moment, and the moment tensor summation procedure that, conversely, does weight the data (Figs 10a′, b′ and c′).

The average focal mechanism of the Mainland Sicily prevalent group (MS1) is reverse with a subordinate strike-slip component (Fig. 10a′); a minor difference in the maximum shortening direction results from applying the Bingham or the moment tensor summation statistics, trend and plunge of the *P*-axis ranging from 144/14 to 133/22.

The average focal mechanism of the Mainland Sicily minor group (MS2) is normal with a subhorizontal E–W trending *T*-axis. (Fig. 10 b′); evidently, to this small group of rather homogenous low-magnitude ($2.0 \leq M_L \leq 3.1$) events, only the Bingham statistics were applied.

The average focal mechanism of the Madonie Mountain group (MM) is normal with a subordinate strike-slip component (Fig. 10c′). The attitude of the maximum stretching direction computed with the Bingham statistics (nearly ENE–WSW subhorizontal *T*-axis) differs $\sim 30^\circ$ from that derived from the moment tensor summation (nearly NNE–SSW subhorizontal *T*-axis); this difference implies that the NNW–SSE normal fault trend characterizes the most frequent low-magnitude events, whereas a nearly E–W fault trend characterizes rarer high-magnitude events.

To compute the seismogenic stress tensor in Mainland Sicily, we performed a stress inversion analysis of a compilation of focal mechanisms composed of two major groups of data. One group consists of all the events analysed in this paper lying within the area in between the OEF and the SBT (Fig. 9a), with the exclusion of only the small MS2 group data set. The MS2 group was excluded because of its kinematic incompatibility with the MS1 group, well highlighted by the dihedral grid construction (Fig. 10), and because of its physically independent geometric position at the SBT footwall (Fig. 9b). The other group consists of the events available in the literature (Table 3) located eastward and westward of the study area, within the boundary of SBT seismogenic province as defined by Lavecchia *et al.* 2007a (grey shaded area in Fig. 11a). This group consists of four events within the westward area (Mazara del Vallo and Belice valley $M_w \geq 4.0$) and of six events within the eastward area (two events with $M_w \geq 4.0$ and four deep Etnean events within $M_w \geq 3.0$; Anderson & Jackson 1987; Frepoli & Amato 2000; Neri *et al.* 2005; Pondrelli *et al.* 2006). The inversion was performed by applying the Gephart & Forsyth (1984) algorithm to a total of 26 events. The computed stress tensor is almost purely compressional, with a nearly horizontal, NNW–SSE trending σ_1-axis (07/341) and a subvertical σ_3-axis attitude (83/152); the shape factor ($R = \sigma_2 - \sigma_1/\sigma_3 - \sigma_1$) equal to 0.6 indicates a near triaxial tensor. The solution gives acceptably constrained stress orientations (the principal axes do not overlap) at the 95 per cent confidence level, with a minimum average misfit $m = 7.4^\circ$.

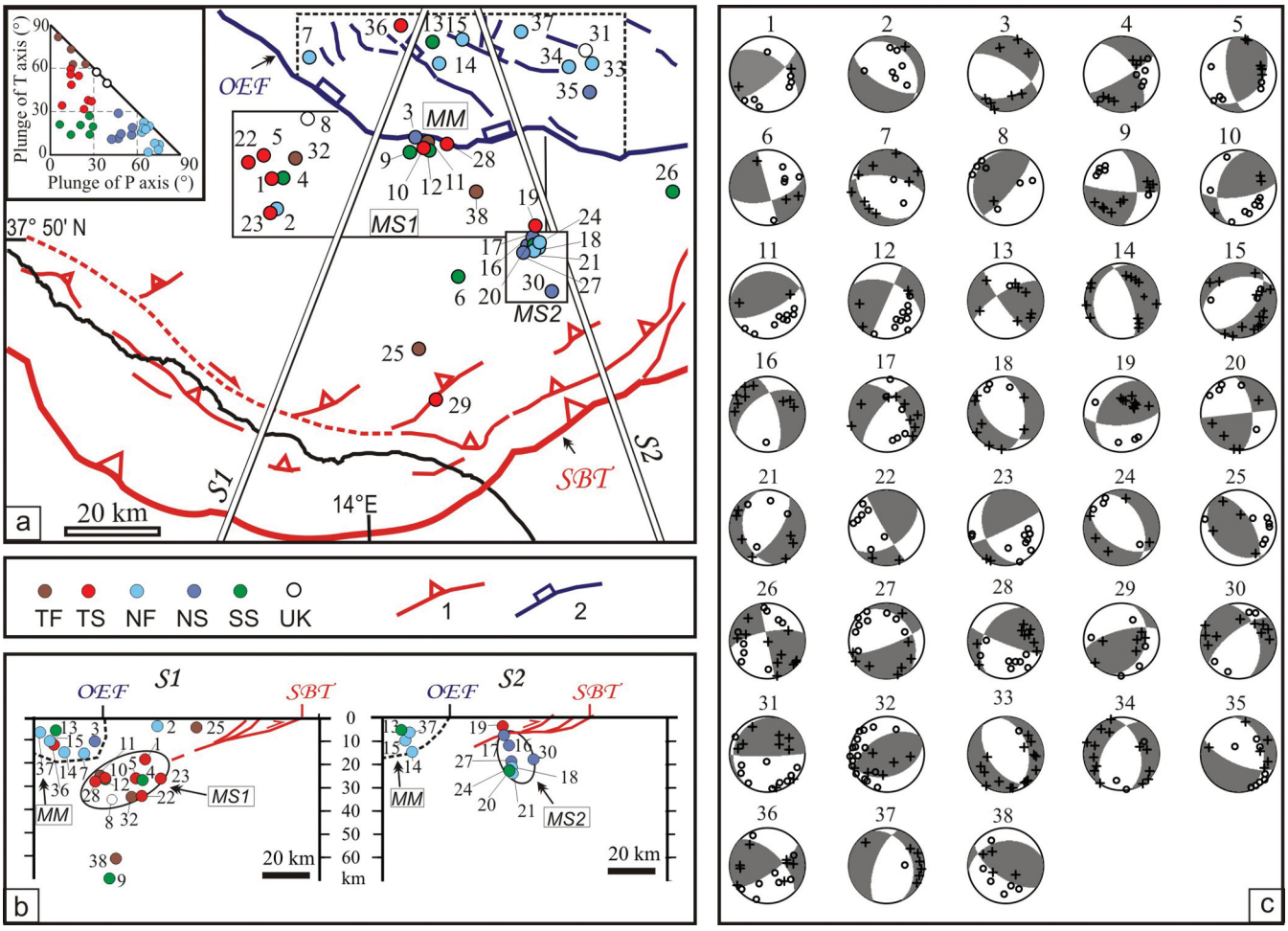

Figure 9. New fault plane solutions in central Sicily. (a) Location map of the focal mechanisms computed in this study. The different colours of the epicentres refer to the kinematic classification as derived from the Frohlich (1992) diagram based on the plunge of *T* and *P* axes (uppermost left side inset); Key: TF, thrust fault; TS, thrust-strike fault; NF, normal fault; NS, normal-strike fault; SS, strike slip; UK, unknown kinematics. The three areas labelled as MS1 (Mainland Sicily 1), MS2 (Mainland Sicily 2) and MM (Madonie Mountains) refer to the grouping of focal mechanisms used in Fig. 10 to compute the average focal solutions. Also shown on the map are the major Plio-Quaternary tectonic structures within the epicentral area: normal and normal-oblique faults in northern Sicily (blue lines), dip-slip and oblique thrust in southern Sicily (red lines). The Outer Extensional Front (OEF) and the Sicilian Basal Trust (SBT) are also indicated. (b) Depth distribution of the new mechanisms projected along the traces of the sections S1 and S2; the hypocentral colours refer to the kinematic classification. (c) New focal mechanism solutions; the source parameters, the quality and the kinematics of the focal mechanisms are listed in Table 3.

7 DISCUSSION

We reevaluated the seismicity and the crustal dynamics of central Sicily, a portion of the Apennine–Maghrebide fold-and-thrust belt not yet well studied from a seismological and seismotectonic point of view, through the analysis of the earthquakes that occurred from 1983 to 2010. The studied data set consists of 392 events, with local magnitudes ranging between 1.0 and 4.7, almost all located at crustal depths. The final relocation, performed in several steps that are discussed in the text, was achieved with standard procedures, but it benefited from the calculation of a new 1-D velocity model for the central portion of Mainland Sicily. Such a model, until now absent from the literature, locates the upper–middle crust, the middle–lower crust and the crust–mantle boundary at depths of 12, 22, and 37 km, respectively, and it defines the corresponding impedance structure well (Fig. 5). The depth value of the Moho discontinuity is in good agreement with those available in the literature that range from a minimum of ∼32 to a maximum of ∼42 km (Cassinis *et al.* 2005 and references therein). In particular, we found the Moho depth to be ∼37 km, which is in good agreement with that defined by Finetti (2005) and confirmed by Tesauro *et al.* (2008) and Grad *et al.* (2009), as well as with that calculated by Chironi *et al.* (2000) from the modelling of the regional pattern of the Bouguer anomaly. This finding is also consistent with the crustal thickness inferred by Lavecchia *et al.* (2007a), as determined by an integrated analysis of tectonic and geophysical data.

The velocity model calculated here for central Sicily, integrated with those from the literature for the surrounding regions (Hybleans, Belice, Etna, Madonie-Peloritani, Aeolian Islands), which are substantially different from a structural-tectonic point of view, was used for the final relocation of the considered seismological data set (Figs 6 and 7C). Such relocation, although improved in quality, still shows a rather diffuse distribution of the seismicity and indicates some previously unrecognized clusters of events. In map view (Fig. 6), one cluster is evident in the NE corner of the study area (Madonie Mountain domain), and the other cluster is

Table 3. Summary of the source parameters of the focal mechanisms computed in this study and available in the literature (A&J87 = Anderson & Jackson 1987; F&A = Frepoli & Amato 2000; P&Al = Pondrelli *et al.* 2004; N05 = Neri *et al.* 2005).

N°	Date	OT	Latitude (°)	Longitude (°)	Depth (km)	M_L	rms (s)	ERH (km)	ERZ (km)	Strike (°)	Dip (°)	Rake (°)	Qf	Qp	N. polar.	N. disc.	Cat.	Ref.
1	19930317	00:07:19.09	37.6233	13.7857	17.46	3.5	0.34	0.8	1.0	50	75	40	A	A	9	0	TS	This study
2	19930327	05:45:30.57	37.5683	13.7972	2.99	2.2	0.39	0.5	0.3	120	65	−100	A	A	8	0	NF	This study
3	19940506	19:09:49.68	37.6785	14.1325	10.83	4.0	0.36	0.4	0.6	65	40	−140	A	B	8	0	NS	This study
4	19950411	12:06:50.80	37.6255	13.8127	26.36	4.1	0.29	0.9	1.0	325	60	−10	B	B	13	2	SS	This study
5	19960713	02:26:02.10	37.6670	13.7675	25.67	3.0	0.66	0.7	0.7	170	65	60	A	B	12	0	TS	This study
6	19990412	05:33:39.95	37.4373	14.2212	6.44	3.9	0.45	0.5	0.6	75	60	0	A	B	8	0	SS	This study
7	20011125	19.34:18.31	37.8490	13.8765	14.84	4.3	0.54	0.7	0.9	137	31	−57	B	B	11	0	NF	This study
8	20020212	17:38:17.60	37.7342	13.8715	34.74	2.6	0.38	0.4	0.4	190	15	60	B	A	8	1	UK	This study
9	20051121	10:57:39.45	37.6700	14.1123	67.62	4.7	0.71	0.5	1.4	0	55	−10	A	B	16	0	SS	This study
10	20080220	14:57:48.25	37.6778	14.1442	25.49	2.7	0.43	0.6	0.5	195	45	30	A	B	12	0	TS	This study
11	20080220	16:40:02.54	37.6890	14.1538	25.38	3.2	0.43	0.3	0.3	65	70	80	A	B	11	0	TF	This study
12	20080220	21:14:24.31	37.6760	14.1485	26.06	3.6	0.40	0.4	0.4	25	90	40	A	B	14	0	SS	This study
13	20080226	16:25:16.95	37.8757	14.1682	4.91	2.4	0.29	0.4	0.5	145	80	160	B	A	9	1	SS	This study
14	20080725	23:42:39.83	37.8355	14.1842	14.41	2.4	0.56	0.5	0.6	195	25	−60	A	A	13	0	NF	This study
15	20080729	09:12:19.34	37.8788	14.2382	9.43	2.9	0.44	0.2	0.5	40	55	−110	B	A	18	1	NF	This study
16	20080828	00:46:53.68	37.4927	14.3842	11.57	2.0	0.48	0.3	0.6	235	50	−30	A	B	10	0	NS	This study
17	20080902	00:28:24.05	37.5202	14.4005	6.00	2.3	0.45	0.3	0.4	220	70	−40	A	A	15	1	NS	This study
18	20080905	00:17:36.33	37.4878	14.4115	21.02	2.2	0.52	0.3	0.4	135	50	−120	A	A	11	0	NF	This study
19	20080905	21:08:55.15	37.5238	14.4037	3.30	2.7	0.53	0.3	0.5	210	40	40	A	B	13	0	TS	This study
20	20080911	06:18:10.76	37.4948	14.3987	22.56	2.5	0.41	0.4	0.5	85	90	−150	A	A	10	0	SS	This study
21	20080915	09:03:47.82	37.4817	14.3998	23.66	2.7	0.47	0.2	0.3	170	35	−130	A	A	11	1	NF	This study
22	20081012	23:53:40.29	37.6542	13.7303	33.25	3.3	0.61	0.5	0.5	150	85	40	A	A	9	0	TS	This study
23	20081128	23:39:21.94	37.5598	13.7800	25.74	4.2	0.81	0.6	0.4	161	40	8	A	B	12	0	TS	This study
24	20081222	21:51:16.61	37.4993	14.4122	22.15	2.6	0.45	0.3	0.4	125	50	−110	A	A	9	0	NF	This study
25	20090426	22:21:28.53	37.3028	14.1277	3.62	2.6	0.46	0.4	0.5	330	60	100	A	A	11	0	TF	This study
26	20090723	00:10:42.14	37.5890	14.7283	24.27	3.3	0.38	0.2	0.3	350	90	−160	A	A	20	1	SS	This study
27	20090801	07:28:35.32	37.4798	14.3738	18.47	2.7	0.61	0.3	0.6	70	80	−120	B	A	17	1	NS	This study
28	20090814	14:55:17.26	37.6998	14.2043	27.00	2.6	0.50	0.2	0.3	210	40	10	B	B	17	1	TS	This study
29	20091004	17:35:55.46	37.2083	14.1648	26.01	2.8	0.60	0.4	0.3	255	70	120	A	A	11	0	TS	This study
30	20091009	07:05:45.51	37.4068	14.4403	17.55	3.1	0.45	0.3	0.5	345	45	−150	B	B	14	0	NS	This study
31	20091028	17:20:01.84	37.8555	14.5297	10.38	2.9	0.56	0.2	0.4	90	85	100	B	A	19	2	UK	This study
32	20091107	07:10:05.13	37.6623	13.8415	33.66	3.9	0.74	0.3	0.3	75	40	100	B	A	23	2	TF	This study
33	20091108	06:51:16.06	37.8312	14.5447	10.00	4.2	0.39	0.2	0.4	350	40	−70	B	A	17	1	NF	This study
34	20091109	19:19:27.58	37.8257	14.4888	10.50	2.5	0.53	0.2	0.3	210	50	−60	B	A	17	1	NF	This study
35	20091205	03:02:41.30	37.7768	14.5385	28.24	3.2	0.51	0.3	0.4	350	35	−40	B	A	14	1	NS	This study
36	20100320	22:52:58.01	37.9062	14.0950	11.04	2.8	0.62	0.4	0.4	315	60	160	B	A	16	2	TS	This study
37	20100404	22:19:15.50	37.9015	14.3788	6.02	2.0	0.37	0.3	0.8	200	65	−70	A	A	8	0	NF	This study
38	20100408	05:06:50.94	37.5958	14.2650	60.34	2.1	0.38	0.6	1.0	260	35	50	B	A	10	1	TF	This study
						M_w												
39	19680115	02:01:00.00	37.7500	12.9830	13.00	5.4	-	-	-	270	50	90	-	-	-	-	TF	A&J87
40	19680116	16:42:00.00	37.8570	12.9760	36.00	5.1	-	-	-	250	58	80	-	-	-	-	TF	A&J87
41	19680125	09:56:00.00	37.6870	12.9660	3.00	5.1	-	-	-	270	64	85	-	-	-	-	TF	A&J87
42	19810622	09:36:00.00	37.6700	12.4700	18.10	4.9	-	-	-	48	29	48	-	-	-	-	TF	P&Al
43	19870813	07:22:00.00	37.9000	15.0600	35.90	4.8	-	-	-	352	42	−10	-	-	-	-	NS	P&Al
44	19880813	12:50:00.00	37.8830	14.9000	26.90	3.4	-	-	-	213	31	161	-	-	-	-	TS	N05
45	19920406	13:08:00.00	37.9000	14.6670	23.30	4.1	-	-	-	60	90	40	-	-	-	-	SS	F&A
46	19931012	20:21:00.00	37.8120	14.8440	23.33	3.6	-	-	-	236	22	−153	-	-	-	-	UK	N05
47	19950210	08:10:00.00	37.6930	14.9690	10.19	3.3	-	-	-	210	54	32	-	-	-	-	TS	N05
48	20001120	23:41:00.00	37.8420	14.9410	23.71	3.3	-	-	-	270	41	102	-	-	-	-	TF	N05

evident in its central portion, north and northwest of Caltanissetta (Mainland Sicily domain). Conversely, two seismic gaps are evident: one in the westernmost sector of the study area, close to the Belice valley area, where the destructive 1968 earthquake occurred, and the other one along the southern coast of Sicily, between Sciacca and Gela, where previous authors (Lavecchia *et al.* 2007a; also the DISS Working Group, http://diss.rm.ingv.it/dissNet/) identified a narrow seismogenic source associated with the shallow portion of the SBT.

Ninety per cent of the relocated earthquakes fall at depths lower than 32 km, the remaining ones being sparsely distributed at depths as great as ∼70 km (see the insets of Fig. 6). A bimodal depth distribution, in terms of not only the number of events and energy release but also prevailing kinematics (histograms in Fig. 10), is well evident. The shallower events are located at depths less than 16 km and therefore are contained mainly within the upper crustal layer; they are mainly due to the extensional seismicity of the Madonie Mountains domain. The deeper ones are located at depths of less

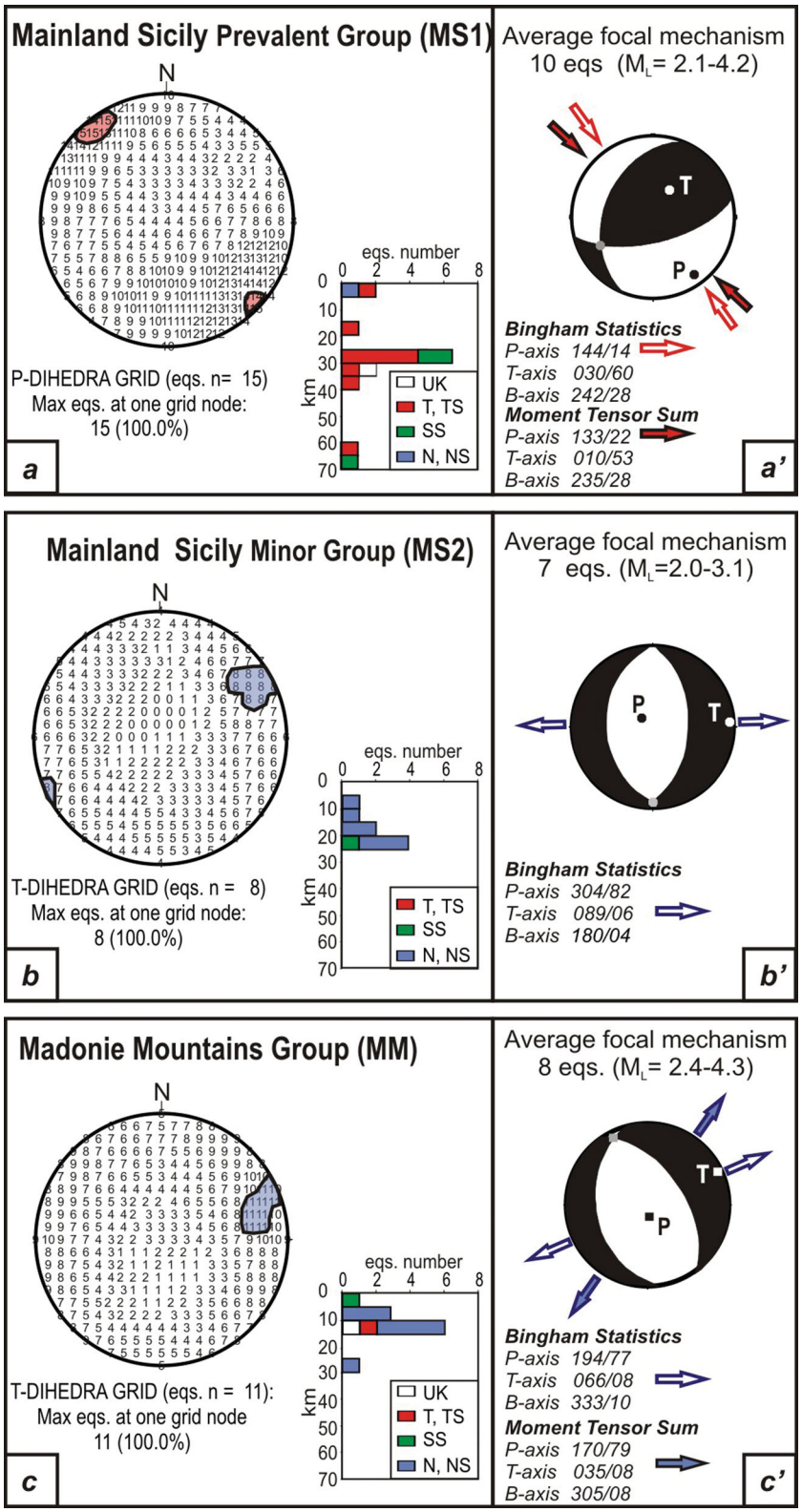

Figure 10. Strain axes and average focal mechanisms in central Sicily. The dihedral grid construction (after Angelier & Mechler 1977) is applied to the three groups of focal mechanisms (MS1, MS2 and MM as in Fig. 9) The red and blue areas in the projection grids (a, b, c) highlight the *P*- and *T*-axes distribution; the histograms report the number of focal mechanisms for each group and the corresponding kinematics versus depths. The average focal mechanisms (a′, b′ and c′) are evaluated with the focal solutions related to the prevalent kinematics in each group, through application of the linked Bingham statistics (data not weighted for seismic moment) and/or of the moment tensor summation. The red and blue arrows represent the maximum shortening and stretching direction, respectively.

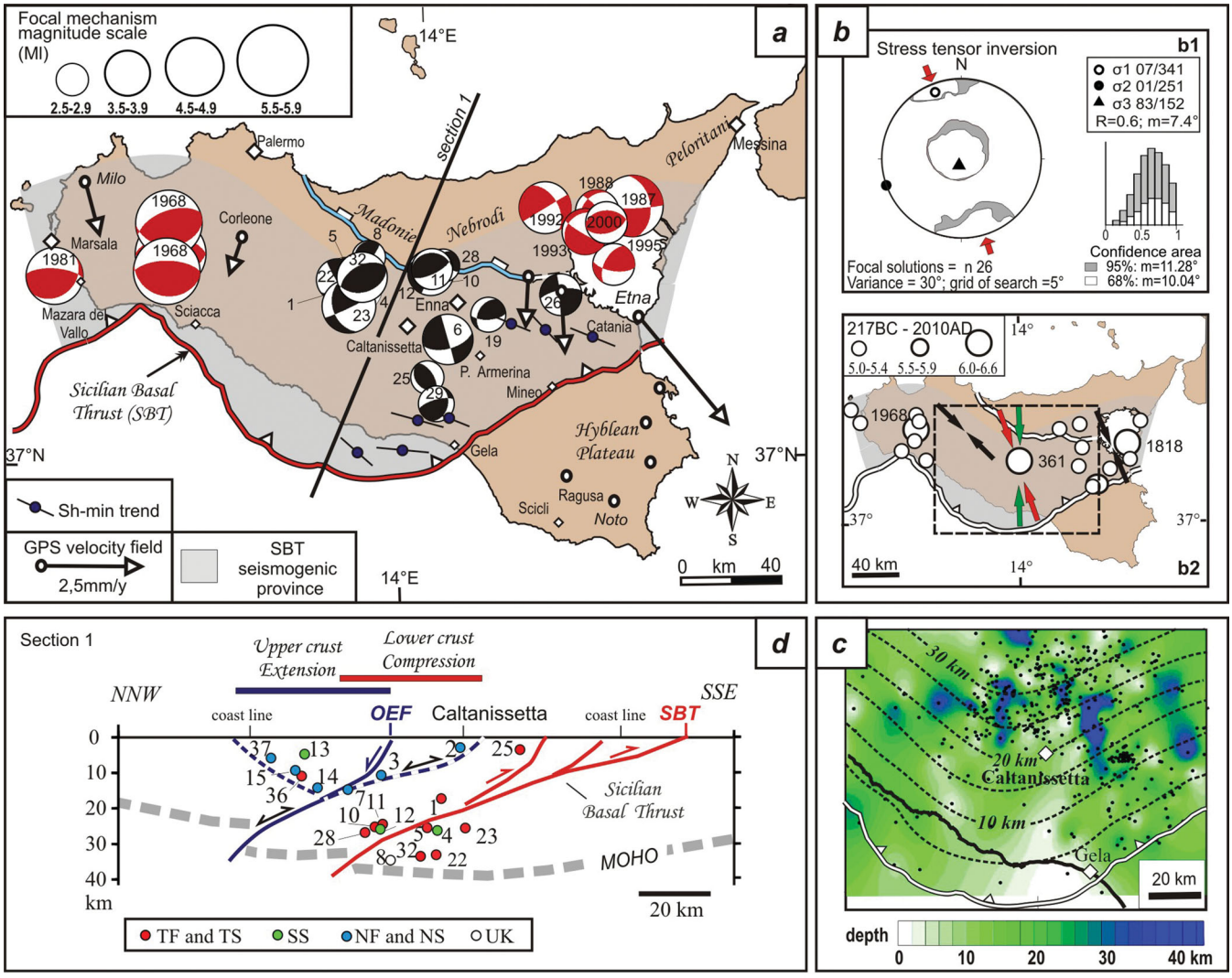

Figure 11. Summary of the results and the seismotectonic interpretation of central Sicily. (a) Distribution of focal mechanisms within the boundary of the SBT seismogenic province (grey transparent area, after Lavecchia *et al.* 2007a). The black beach balls are the new focal mechanisms computed in this study; the red ones are those available in the literature (see text and Table 3). The black arrows represent the velocity field measured from continuous GPS stations within the boundary of the SBT seismogenic province with respect to fixed sites (white circles) within the Hyblean foreland (from Devoti *et al.* 2011); the shear-minimum (Sh_{min}) axes refer to the borehole breakout data (from Montone *et al.* 2004). (b) Stress tensor inversion results from the 26 focal mechanisms reported on the map. (b1) Stereographic lower-hemisphere projection of the best-fitting principal stress axes (σ_1, σ_2 and σ_3) and of their 68 and 95 per cent confidence ranges; the histogram refers to the distribution of the number of tested stress models within the 68 and 95 per cent confidence ranges referring to the dimensionless R shape factor. (b2) Comparison among the calculated minimum principal stress axis (σ_1; red arrows in b1 and b2) are the ones proposed by Neri *et al.* (2005) (black arrows) and the direction of the horizontal contractional component of the average strain tensor computed by Visini *et al.* (2010) (green arrows). The epicentres (white circles) of the historical and instrumental earthquakes with $M_w \geq 5.0$ and depths $\leq$40 km located within the boundary of the SBT seismogenic province are also reported. (c) Contour depth lines of the central Sicily final relocations compared with the contour depth lines of the Sicilian Basal Thrust as reconstructed by Lavecchia *et al.* 2007a. (d) Interpretative depth view of the central Sicily seismicity; the hypocentres of the focal mechanisms computed in this paper, coloured on the basis of their kinematics (see key in Fig. 9), are projected along the trace of Section 1 and compared with the crustal geometry of the major tectonic structures as interpreted by Lavecchia *et al.* 2007(a).

than 32 km and therefore are contained mainly within the lower crustal layer; they are substantially related to the Mainland Sicily compressional seismicity (MS1 domain in Fig. 9).

The northward deepening of the relocated earthquakes, evident in the section view of Fig. 7(C) and in the earthquake depth contour areas of Fig. 11(c), recalls the northward deepening of the SBT, whose depth contour lines were reconstructed by Lavecchia *et al.* (2007a). When overlapping the hypocentral distribution of the here calculated focal mechanism with the extrapolation at depth of the SBT, the control exerted by such a still-active tectonic feature on the earthquake distribution is very well evident (Figs 9b, 11c and 11d). In fact, the compressional seismicity of Mainland Sicily (MS1 domain) lies just in the surroundings of the SBT plane, at mid- to lower-crustal depths and within its hangingwall. Conversely, the isolated small extension cluster of the MS2 domain clearly lies within the SBT footwall (Fig. 9b) and recalls other small, strike-slip

and normal deformation volume, recorded in the Hyblean forelands at the focal depth of 17–25 km below the active thrust zone of the Sicily mountain chain (Scarfì *et al.* 2003).

The coexistence of seismogenic extension in the Madonie domain at upper crustal depths ($< \sim$15 km) and of compression in mainland Sicily at mid-to-lower crustal depths, with areas of partial geometric overlap between the two (Fig. 11d), recalls the distribution of the seismogenic province in central Italy, where the pede-Apennine NNW–SSE striking mid-to-deep crustal thrust structures coexist in the same area with the shallower and coaxial Apennine extensional faults and deepens beneath them (Lavecchia *et al.* 2003; Lavecchia *et al.* 2007b).

Whether the maximum NNW–SSE average shortening direction computed in this paper in Mainland Sicily (Fig. 10a′) is coaxial with the average Madonie maximum stretching direction (Fig. 10b′) is not clear from the analysis of our focal mechanisms. In fact, a nearly WSW–ENE trend of *T*-axis is obtained when applying the Bingham statistics whereas an average NNE–SSW trend is obtained when weighting more the largest events. Both directions are partially supported when considering outside data. The WSW–ENE trend of *T*-axis is consistent with the tensional strain pattern from GPS data reported by Cuffaro *et al.* (2011) and with field fault slip data reported by Billi *et al.* (2010) and Barreca *et al.* (2010). Conversely, the NNE–SSW direction is subparallel with *T*-axes derived from RCMT focal mechanisms (Pondrelli *et al.* 2006) and from geodetic data reported by Devoti *et al.* (2011). More information is needed to underscore the true meaning of this observed contradiction, but what is certainly confirmed is the existence of an extensional domain in northeastern Sicily, as proposed by Lavecchia *et al.* 2007a, b and by Billi *et al.* 2010.

The compressional tectonic pattern defined in Mainland Sicily from the new focal mechanisms (black beach balls in Fig. 11a), which is almost purely compressive with a NNW–SSE oriented *P*-axis, is consistent with all the available information (red beach balls in Fig. 11a). In fact, it is similar to the fault plane solutions of the Belice 1968 sequence (M_w 6.1) and to the 1981 Mazara earthquake (M_w 4.9), which occurred in western Sicily, as well as to the average focal mechanism computed with small magnitude events located at middle and lower crustal depths beneath the Etna edifice (Visini *et al.* 2010). The stress inversion of all the focal mechanisms falling within the boundary of the SBT province (transparent grey in Fig. 11a) has further demonstrated the presence of a largely homogenous NNW–SSE compressive stress field (Fig. 11b). The obtained tensor is consistent with the ones previously inverted from focal mechanisms by Neri *et al.* (2005), as well as with the principal strain axes evaluated by Visini *et al.* (2010). Moreover, the oblique convergence of central Sicily relative to the GPS site Noto, within the Hyblean Foreland, was noted by Ferranti *et al.* (2008). More recently, on the basis of geodetic data, Devoti *et al.* (2011) computed an active NNW–SSE convergence of $\sim$1.1 $\pm$ 0.2 mm yr^{-1} between the Mainland Sicilian domain and the Hyblean–Malta Plateau, and they also noted a slight subsidence of the rigid plateau block (0.2 $\pm$ 0.2 mm yr^{-1}), opposed to an uplift of 1.2 $\pm$ 0.5 mm yr^{-1} in northwestern Sicily. Such a deformation pattern well supports the hypothesis of the active thrusting of Mainland Sicily above the SBT.

The active compressional activity in Mainland Sicily (Fig. 11b) is nearly coaxial to that of the E–W striking compressional domain offshore of northern Sicily (Fig. 1). Some authors have interpreted the latter as proof of a backward shift of the Sicilian Apennine–Maghrebian active thrust front and for a definitive abandonment of the SBT emerging along the Sciacca–Gela–Catania thrust front (Chiarabba *et al.* 2005). Other authors consider the compressional strip as an independent process, because of an incipient southward dipping subduction of the Tyrrhenian thinned lithosphere beneath the Sicilian crust (Goes *et al.* 2004; Billi *et al.* 2007). Available data do not allow the problem to be solved unequivocally. Seismological and geodetic data show clearly that the offshore strip and the Mainland Sicily domains are separated by the interposed northern Sicily Madonie–Nebrodi–Peloritani extensional belt (Devoti *et al.* 2011 and references therein); therefore, the hypothesis of a large active compressional domain from to southern Tyrrhenian to southern Sicily (Jenny *et al.* 2006) can be reasonably excluded. We suggest that two compressional domains, although coaxial, would be an expression of two different geodynamic processes: the compressive strip offshore northern Sicily would absorb most of the convergence rate between the convergent Nubia and Eurasia plates, whereas the Mainland Sicily compression domain, at the outer front of the Apennine–Maghrebides fold-and-thrust belt, and the northern Sicily extensional domain might represent a still-ongoing activity of the outward moving Tyrrhenian–Apennine extension–compression pair, which since late Miocene times has been responsible for coeval inward extension and outward compression at a crustal scale (Lavecchia 1988).

8 CONCLUSIONS

This paper provides new data and insight to better understand the seismicity and tectonic framework of central Sicily. The computation of a new 1-D velocity model through the inversion of seismic data, the relocation of events by using the new model and the computation of focal mechanisms have especially contributed to suggest the importance of the geometry and the seismogenic role played by the SBT, the outermost thrust of the outward-verging Apennine–Maghrebian thrust system. The SBT deepens at a low-angle (average 30°) northward, cross-cutting the middle–lower crustal transition (22 km) approximately beneath Caltanissetta and reaching the Moho discontinuity at depth of $\sim$ 35 km, beneath the southern portion of the Madonie Mountains domain (Fig. 11d). The data analysed in this paper show that the seismogenic thrust is located mainly at mid-to-lower crustal depths between 20 and 32 km, thus helping to confirm the thick-skinned configuration of the active thrust structure at the outermost Sicilian front. Such configuration, already proposed in the literature (Guarnieri *et al.* 2002 and Lavecchia *et al.* 2007a), also fits well with a crustal reflection seismic profile recently recorded across central Sicily by Accaino *et al.* (2010), from the Tyrrhenian shore to the Sicily Channel.

In the recent literature (Basili *et al.* 2008; Meletti *et al.* 2008), as well as in the seismic zonation of the Italian territory that is available online (Working Group DISS 2010), the earthquake potential on the SBT is still largely under evaluated. The Mainland Sicily territory, which is located along the surface projection of the lower crustal portion of the SBT, is classified as an 'aseismic region', and a narrow compressional zone characterizes only the shallow portion of the SBT along the Sciacca–Gela–Catania front in Southern Sicily. Our results show that a large seismogenic province, here called SBT province (grey transparent area in Fig. 11a), is undergoing homogenous NNW–SSE compressive stress, at the hangingwall of the SBT, with most of the seismic shearing being released just along the basal thrust plane in the 20–35 km depth interval. Such results, although still not fully accepted in the literature, which sometimes considers the SBT and the associated splays as an abandoned structure (Chiarabba *et al.* 2005), are fully supported by geodetic data, which indicate the SSE-verging thrusting of Mainland Sicily at

relevant geodetic rates (Devoti *et al.* 2011). The implications in terms of seismic hazard assessment are evident as, in historical times, the SBT has been capable of releasing at least three large earthquakes with $M_w \geq 6.0$ (361, 1818, 1968; Fig. 1a) and several more moderate events (Lavecchia *et al.* 2007a). The theory of a possible association with the highly destructive 1693 earthquake (Fig. 1a) of eastern Sicily (Io = XI MCS) (Visini *et al.* 2009) should also be considered.

ACKNOWLEDGMENTS

We thank the Editor Ingo Grevemeyer and the two anonymous reviewers for the constructive remarks that greatly improved the work. We also thank Paolo Boncio, Paolo Favali and Stephen Monna for their valuable comments and discussions.

REFERENCES

Accaino, F. *et al*., 2010. A crustal seismic profile across Sicily, *Tectonophysics,* **508,** 52–61, doi:10.1016/j.tecto.2010.07.011.

Allmendinger, R.W., 2001. FaultKinWin version 1.1; a program for analyzing fault slip data for Windows^{TM} computers. Available at: ftp://www.geo.cornell.edu/pub/rwa/.

Amato, A. & Mele, F.M., 2008. Performance of the INGV National Seismic Network from 1997 to 2007, *Ann. Geophys.,* **51**(2–3), 417–431.

Anderson, D.L. & Jackson, J., 1987. Active tectonics of the Adriatic region, *Geophys. J. R. astr. Soc.,* **91,** 937–983.

Angelier, J. & Mechler, P., 1977. Sur une mèthode graphique de recherche des contraintes principales également utilisable en tectonique et en sèismologie: la méthode des diédres droits, *Bull. Soc. Géol. Fr.,* **19,** 1309–1318.

Azzaro, R., Barbano, M.S., Antichi, B. & Rigano, R., 2000. Macroseismic catalogue of Mt. Etna earthquakes from 1832 to 1998, *Acta Vulcanol.,* **12,** 3–36 and CDROM.

Bagh, S., Chiaraluce, L., De Gori, P., Moretti, M., Govoni, A., Chiarabba, C., Di Bartolomeo, P. & Romanelli, M., 2007. Background seismicity in the Central Apennine of Italy: the Abruzzo region case study, *Tectonophysics,* **444,** 80–92.

Barberi, G., Cosentino, M.T., Gervasi, A., Guerra, I., Neri, G. & Orecchio, B., 2004. Crustal seismic tomography in the Calabrian Arc region, south Italy, *Phys. Earth planet. Inter.,* **147,** 297–314.

Barreca, G., Barbano M.S., Carbone S. & Monaco C., 2010. Archaeological evidence for Romanage faulting in central-northern Sicily: Possible effects of coseismic deformation, *Geol. Soc. Am. Spec. Papers,* **471,** 223–232, doi:10.1130/2010.2471(18).

Basili, R., Valensise, G., Vannoli, P., Burrato, P., Fracassi, U., Mariano, S., Tiberti, M.M. & Boschi, E., 2008. The Database of Individual Seismogenic Sources (DISS), version 3: summarizing 20 years of research on Italy's earthquake geology, *Tectonophysics,* **453,** 20–43.

Billi, A., Presti, D., Faccenna, C., Neri, G. & Orecchio, B., 2007. Seismotectonics of the Nubia plate compressive margin in the south-Tyrrhenian region, Italy: clues for subduction inception, *J. geophys. Res.,* **112**(B08302), 907, doi:10.1029/2006JB004837.

Billi, A., Presti, D., Orecchio, B., Faccenna, C. & Neri, G., 2010. Incipient extension along the active convergent margin of Nubia in Sicily, Italy: Cefalù-Etna seismic zone, *Tectonics,* **29,** TC4026, doi:10.1029/2009TC002559.

Butler, R.W.H., Grasso, M. & La Manna, F., 1992. Origin and deformation of the Neogene—Recent Maghrebian foredeep at the Gela Nappe, SE Sicily, *J. Geol. Soc. Lond.,* **149,** 547–556.

Cassinis, R., Scarascia, S. & Lozej, A., 2005. Review of seismic wide-angle reflection–refraction (WARR) results in the Italian region (1956–1987), in *CROP PROJECT: Deep Seismic Exploration of the Central Mediterranean and Italy,* pp. 31–56, ed. Finetti, I.R., Elsevier, Amsterdam.

Castello, B., Selvaggi, G., Chiarabba, C. & Amato, A., 2005. CSI Catalogo della sismicità italiana 1981–2002. Versione 1.0 (INGV-CNT, Roma). Available at: http://csi.rm.ingv.it/.

Catalano, R., Di Stefano, P., Sulli, A. & Vitale, F.P., 1996. Paleogeography and structure of the central Mediterranean: Sicily and its offshore area, *Tectonophysiscs,* **260,** 291–323.

Catalano, S., Torrisi, S. & Ferlito, C., 2004. The relationship between Late Quaternary deformation and volcanism of Mt. Etna (eastern Sicily): new evidence from the sedimentary substratum in the Catania region, *J. Volc. Geotherm. Res.,* **132,** 311–334.

Chiarabba, C. & Frepoli, A, 1997. Minimum 1D velocity models in Central and Southern Italy: a contribution to better constrain hypocentral determinations, *Annali di Geofisica,* **XL**(4), 937–954.

Chiarabba, C., Jovane, L. & Di Stefano, R., 2005. A new view of Italian seismicity using 20 years of instrumental recordings, *Tectonophysics,* **395,** 251–268.

Chiarabba, C., Piccinini, D. & De Gori, P., 2009. Velocity and attenuation tomography of the Umbria Marche 1997 fault system: evidence of a fluid-governed seismic sequence, *Tectonophysics,* **476,** 73–84.

Chironi, C., De Luca, L., Guerra, I., Luzio, D., Moretti, A., Vitale, M. & Sealand Group, 2000. Crustal stuctures of the Tyrrhenian Sea and Sicily Channel on the basis of the M25, M26, M28, M39 WARR profiles, *Boll. Soc. Geol. Ital.,* **119,** 189–203.

Cocina, O., Neri, G., Privitera, E. & Spampinato, S., 1997. Stress tensor computations in the Mount Etna area (southern Italy) and tectonic implications, *J. Geodyn.,* **23,** 109–127.

Cuffaro, M., Riguzzi, F., Scrocca, D. & Doglioni, C., 2011. Coexisting tectonic settings: the example of the southern Tyrrhenian Sea, *Int. J. Earth Sci. (Geol. Rundsch.),* **100,** 1915–1924, doi:10.1007/s00531-010-0625-z.

D'Agostino, N. & Selvaggi, G., 2004. Crustal motion along the Eurasia-Nubia plate boundary in the Calabrian Arc and Sicily and active extension in the Messina Straits from GPS measurements, *J. geophys. Res.,* **109,** B11402, doi:10.1029/2004JB002998.

Del Pezzo, E., Maresca, R., Martini, M. & Scarpa, R., 1984. Seismicity of the Aeolian Islands, Southern Italy, *Ann. Geophysicae,* **2**(2), 173–180.

Devoti, R., Esposito, A., Pietrantonio, G., Pisani, A.R. & Riguzzi, F., 2011. Evidence of large scale deformation patterns from GPS data in the Italian subduction boundary, *Earth planet. Sci. Lett.,* **311**(3–4), doi:10.1016/j.epsl.2011.09.034.

Eberhart-Phillips, D. & Michael, A.J., 1993. Three-dimensional velocity structure, seismicity, and fault structure in the Parkfield region, central CA, *J. geophys. Res.,* **98,** 15737–15758.

Ferranti, L. *et al*., 2008. Active deformation in southern Italy, Sicily and southern Sardinia from GPS velocities of the peri-tyrrhenian geodetic array (PTGA), *Boll. Soc. Geol. It.,* **127,** 299–316.

Finetti, I.R., 2005. Depth contour Map of the Moho discontinuity in the Central Mediterranean region from new CROP seismic data, in *CROP Project, Deep Seismic Exploration of the Central Mediterranean and Italy,* pp. 597– 606, ed. Finetti, I. R., Elsevier, New York, NY.

Finetti, I. & Del Ben, A., 1986. Geophysical study of the Tyrrhenian opening, *Bull. Geofis. Teor. Appl.,* **XXVIII**(110), 75–152.

Frepoli, A. & Amato, A., 2000. Fault Plane Solutions of Crustal Earthquakes in Southern Italy (1988–1995): seismotectonic Implications, *Ann. Geofis.,* **43,** 437–467.

Frohlich, C., 1992. Triangle diagrams: ternary graphs to display similarity and diversity of earthquake focal mechanisms, *Phys. Earth planet. Inter.,* **75,** 193–198.

Gasparini, C., Iannaccone, G. & Scarpa, R., 1985. Fault-plane solutions and seismicity of the Italian Peninsula, *Tectonophysics,* **117,** 59–78.

Gasperini, P., Bernardini, F., Valensise, G. & Boschi, E., 1999. Defining seismogenic sources from historical earthquake felt reports, *Bull. seism. Soc. Am.,* **89,** 94–110.

Gephart, J.W. & Forsyth, D.W., 1984. An improved method for determining the regional stress tensor using earthquake focal mechanism data: application to San Fernando earthquake sequence, *J. geophys. Res.,* **89,** 9305–9320.

Ghisetti, F. & Vezzani, L., 1984. Thin-skinned deformations of the western Sicily thrust belt and relationships with crustal shortening; mesostructural data on the Mt. Kumeta–Alcantara fault zone and related structures, *Boll. Soc. Geol. Ital.,* **103,** 129–157.

Ghisetti, F.C., Gorman, A.R., Grasso, M. & Vezzani, L., 2009. Imprint of foreland structure on the deformation of a thrust sheet: the plio-pleistocene Gela Nappe (southern Sicily, Italy) (2009), *Tectonics,* **28,** TC4015, doi:10.1029/2008TC002385.

Goes, S., Jenny, S., Hollenstein, C., Kahle, H.G. & Geiger, A., 2004. A recent tectonic reorganization in the south-central Mediterranean, *Earth planet. Sci. Lett.,* **226,** 335–345.

Grad, M., Tiira, T. & ESC Working Group, 2009. The Moho depth map of the European Plate, *Geophys. J. Int.,* **176,** 279–292, doi:10.0000/j.1365-246X.2008.03919.x.

Guarnieri, P., Carbone, S. & Di Stefano, A., 2002. The Sicilian orogenic belt: a critical tapered wedge? *Boll. Soc. Geol. Ital.,* **121,** 221–230.

Guidoboni, E., Muggia, A., Marconi, C. & Boschi, E., 2002. A Case Study in Archaeoseismology. The Collapses of the Selinunte Temples (Southwestern Sicily): two Earthquakes Identified, *Bull. seism. Soc. Am.,* **92,** 2961–2982.

Hirn, A., Nercessian, A., Sapin, M., Ferrucci, F. & Wrrtlinger, G., 1991. Seismic heterogeneity of Mt. Etna: structure and activity, *Geophys. J. Int.,* **105,** 139–153.

ISB Italian Seismic Bulletin, 2003–2010. Available at: http://bollettinosismico.rm.ingv.it/.

Jenny, S., Goes, S., Giardini, D. & Kahle, H.G., 2006. Seismic potential of Southern Italy, *Tectonophysics,* **415,** 81–101.

Kissling, E., 1995. *Velest Users Guide,* pp. 26, Internal report Institute of Geophysics, ETH Zurich.

Kissling, E., Ellsworth, W.L., Eberhart-Phillips, D. & Kradolfer, U., 1994. Initial reference models in local earthquake tomography, *J. geophys. Res.,* **99,** 19635–19646.

Lahr, J.C., 1989. HYPOELLIPSE/version 2.0: a computer program for determining local earthquake hypocentral parameters, magnitude, and first motion pattern, *U.S. Geol. Surv., Open File Rep.*, **95,** 89–116.

Langer, H., Raffaele, R., Scaltrito, A. & Scarfi, L., 2007. Estimation of an optimum velocity model in the Calabro-Peloritan mountains – assessment of the variance of model parameters and variability of earthquake locations, *Geophys. J. Int.,* **170,** 1151–1164, doi:10.1111/j.1365-246X.2007.03459.x.

Lavecchia, G., 1988. The Tyrrhenian-Apennines system: structural setting and seismotectogenesis, *Tectonophysics,* **147,** 263–296.

Lavecchia, G., Boncio, P. & Creati, N., 2003. A lithospheric scale thrust zone as an explanation for the relatively deep seismicity of central Italy, *J. Geodyn.,* **36,** 79–94.

Lavecchia, G., Ferrarini, F., de Nardis, R., Visini, F. & Barbano, S., 2007a. Active thrusting as a possible seismogenic source in Sicily (Southern Italy): some insights from integrated structural-kinematic and seismological data, *Tectonophysics,* **445,** 145–167.

Lavecchia, G., de Nardis, R., Visini, F., Ferrarini, F. & Barbano, S., 2007b. Seismogenic evidence of ongoing compression in eastern-central Italy and mainland Sicily: a comparison, *Boll. Soc. Geol. It.,* **126,** 209–222.

Lentini, F., Carbone, S. & Catalano, S., 1994. Main structural domains of the central Mediterranean region and their Neogene tectonic evolution, *Boll. Geofis. Teor. Appl.,* **36,** 103–125.

Lickorish, W.H., Grasso, M., Butler, R.W.H. & Argnani, A., 1999. Structural styles and regional tectonic setting of the Gela "Nappe" and frontal part of the Maghrebian thrust belt in Sicily, *Tectonics,* **18,** 655–668.

Maggi, C., Frepoli, A., Cimini, G.B., Console, R. & Chiappini, M., 2010. Recent seismicity and crustal stress field in the Lucanian Apennines and surrounding areas (Southern Italy): seismotectonic implications, *Tectonophysics,* **463,** 130–144.

McKenzie, D., 1972. Active Tectonics of the Mediterranean Region, *Geophys J. R. astr. Soc.,* **30,** 109–185.

Meletti, C., Galdini F., Valensise G., Stucci M., Basili R., Barba S., Vannucci G. & Boschi E., 2008. A seismic source model for the seimic hazard assessment of the Italian territory, *Tectonophysics,* **450,** 85–108.

Monaco, C., Mazzoli, S. & Tortorici, L., 1996. Active thrust tectonics in western Sicily (Southern Italy): the 1968 Belice earthquake sequence, *Terra Nova,* **8,** 372–381.

Monna, S., Filippi, L., Beranzoli L. & Favali, P., 2003. Rock properties of the upper-crust in Central Apennines (Italy) derived from high-resolution 3-D tomography, *Geophys. Res. Lett.,* **30**(7), 1408, doi:10.1029/2002GL016780.

Montone, P., Mariucci, M.T., Pondrelli, S. & Amato A., 2004. An improved stress map for Italy and surrounding regions (Central Mediterranean), *J. geophys. Res.,* **109,** B10410, doi:10.1029/2003JB002703.

Musumeci, C., Di Grazia, G. & Gresta, S., 2003. Minimum 1-D velocity model in Southeastern Sicily (Italy) from local earthquake data: an improvement in location accuracy, *J. Seismol.,* **7,** 469–478.

Neri, G., Barberi, G., Oliva, G. & Orecchio, B., 2005. Spatial variation of seismogenic stress orientations in Sicily, South Italy, *Phys. Earth planet. Inter.,* **148,** 175–191.

Piccinini, D., Piana Agostinetti, N., Roselli, P., Ibs-von Seht, M. & Braun, T., 2009. Analysis of small magnitude seismic sequences along the Northern Apennines (Italy), *Tectonophysics,* **476,** 136–144.

Pondrelli, S., Piromallo, C. & Serpelloni, E., 2004. Convergence vs. retreat in Southern Tyrrhenian Sea: insights from kinematics, *Geophys. Res. Lett.,* **31,** 6, doi:10.1029/2003GL019223.

Pondrelli, S., Salimbeni, S., Ekström, G., Morelli, A., Gasperini, P. & Vannucci, G., 2006. The Italian CMT dataset from 1977 to the present, *Phys. Earth planet. Inter.,* **159,** 286–303.

Reasenberg, P. & Oppenheimer, D., 1985. FPFIT, FPPLOT and FPPAGE: FORTRAN computer programs for calculating and dislaying earthquake fault-plane solutions, *U.S. Geol. Surv., Open File Rep.*, 85–739.

Richter, C.F., 1958. *Elementary Seismology,* W.H. Freeman and Company, San Francisco, CA.

Scarfì, L., Langer, H. & Gresta, S., 2003. High precision relative locations of two microearthquake clusters in Southeastern Sicily, Italy, *Bull. seism. Soc. Am.,* **934,** 1479–1497.

Schorlemmer, D., Mele, F. & Marzocchi, W., 2010. A completeness analysis of the National Seismic Network of Italy, *J. geophys. Res.,* **115,** B04308, doi:10.1029/2008JB006097.

Tavarnelli, E., Renda, P., Pasqui, V. & Tramutoli, M., 2003. The effects of post-orogenic extension on different scales; an example from the Apennine–Maghrebide fold-and-thrust belt, SW Sicily, *Terra Nova,* **15,** 1–7.

Tesauro, M., Kaban, M.K. & Cloetingh, S.A.P.L, 2008. EuCRUST-07: a new reference model for the European crust, *Geophys. Res. Lett.,* **35,** L05313, doi:10.1029/2007GL032244.

Thurber, C.H., 1992. Hypocenter-velocity structure coupling in local earthquake tomography, *Phys. Earth planet. Inter.,* **75,** 55–62.

Torelli, L., Grasso, M., Mazzoldi, G. & Peis, D., 1998. Plio-Quaternary tectonic evolution and structure of the Catania foredeep, the northern Hyblean Plateau and the Ionian shelf (SE Sicily), *Tectonophysics,* **298,** 209–221.

Valensise, G. & Pantosti, D., 2001. The investigation of potential earthquake sources in peninsular Italy: a review, *J. Seismol.,* **5,** 287–306.

Visini, F., de Nardis, R., Barbano, M. S. & Lavecchia, G., 2009. Testing the seismogenic sources of the January 11th 1693 Sicilian earthquake (Io X/XI): Insights from macroseismic field simulations, *Boll. Soc. Geol. It.,* **128,** 147–156.

Visini, F., de Nardis, R. & Lavecchia, G., 2010. Rates of active compressional deformation in central Italy and Sicily: evaluation of the seismic budget, *Int. J. Earth Sci. (Geol Rundsch),* **99**(Suppl. 1), 243–264.

Working Group CPTI, 2004. Catalogo Parametrico dei Terremoti Italiani, version 2004 (CPTI04). INGV, 1052 Bologna. Available at: http://emidius.mi.ingv.it/CPTI/.

Working Group DISS, 2010. Database of Individual Seismogenic Sources (DISS), Version 3.1.1: A compilation of potential sources for earthquakes larger than *M* 5.5 in Italy and surrounding areas, http://diss.rm.ingv.it/diss/.